https://www.aimspress.com/journal/mine

Mathematics in Engineering, 8(2): 209–268.
DOI:10.3934/mine.2026008
Received: 04 September 2025
Revised: 07 March 2026
Accepted: 10 March 2026
Published: 25 March 2026

Research article

Elastoplasticity with softening as a state-dependent sweeping process: non-uniqueness of solutions and emergence of shear bands in lattices of springs†

Ivan Gudoshnikov*

Institute of Mathematics of the Czech Academy of Sciences, Žitná 25, 110 00, Praha 1, Czech Republic

† **This contribution is part of the Special Issue:** Multi-Rate Processes and Hysteresis
Guest Editors: Menita Carozza; Dmitrii Rachinskii; Ciro Visone
Link: www.aimspress.com/mine/article/6692/special-articles

* **Correspondence:** Email: gudoshnikov@math.cas.cz.

Abstract: Plasticity with softening and fracture mechanics lead to ill-posed mathematical problems due to the loss of monotonicity. Multiple co-existing solutions are possible when softening elements are coupled together, and solutions cannot be continued beyond the point of complete degradation of the set of admissible stresses. We present a state-dependent sweeping process which solves the evolution of elasto-plastic Lattice Spring Models with arbitrary placement of softening, hardening and perfectly plastic springs. Using numerical simulations of regular grid lattices with softening, we demonstrate the emergence of non-symmetric shear bands with strain localization. At the same time, in toy examples it is easy to analytically derive multiple co-existing solutions. These solutions correspond to fixed points in the implicit catch-up algorithm and we observe a discontinuous bifurcation with the exchange of stability of those fixed points.

Keywords: state-dependent sweeping process; quasi-variational inequalities; plasticity with softening; non-uniqueness of solutions; shear band; strain localization

1. Introduction

Modeling of the plastic deformation process is an important scientific pursuit due to numerous practical applications, e.g., in manufacturing, construction and transportation industries. Different materials and phenomena are described by different models and their mathematical complexity varies significantly.

We focus on rate-independent elastoplasticity models, which can be divided into *strain hardening*, *perfect plasticity* and *strain softening* types, classified by observed stress response to imposed deformation. In this text we develop a finite-dimensional in space and continuous in time model, which covers all three types in a uniform manner. In such a model, the transition between these qualitatively different types is due to a quantitative change of parameters, which paves the way for a mathematical study of this bifurcation. Now let us provide an introduction on the three types of plasticity to explain their qualitative differences, as well as the mathematical results and challenges associated with each type.

To begin, we illustrate the plastic behaviors with a simple example of a one-dimensional elasto-plastic spring. Let the spring be linearly elastic with stiffness $k > 0$ near its stress-free state, and impose a prescribed monotonically increasing elongation $l(t)$ on the spring (Figure 1a). Assume that this model is quasi-static (this applies to all models in the paper).

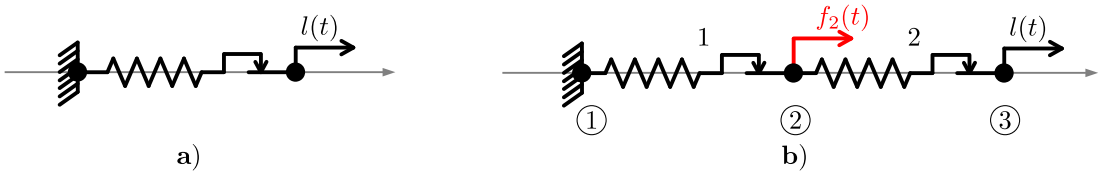

Figure 1. a) An elasto-plastic spring with the displacements of its left and right endpoints prescribed to be 0 and $l(t)$, respectively. b) A model of two elasto-plastic springs connected in series with displacements 0 and $l(t)$ prescribed for the nodes ① and ③, respectively, and a prescribed force $f_2(t)$, applied to the node ②.

1.1. Perfect plasticity

The simplest to construct is the model of a *perfectly plastic* material, with the *yield limit* c_0 being the only material parameter apart from k. At all times the stress σ must stay in the *set of admissible stresses*:

$$\sigma \in [-c_0, c_0] \tag{1.1}$$

(we limit the scope of the paper to *isotropic* plasticity, which means that the sets of admissible stresses are symmetric with respect to 0). After the stress reaches a yield limit, all further elongation contributes to progressive plastic deformation, but the stress remains constant (Figure 2a).

Such simplicity is, however, deceptive, because the elongation-stress relation (or, in the case of continuous media, the strain-stress relation) is non-injective, which causes plenty of complications. If we connect just two elastic-perfectly plastic springs in series to make a slightly more complex model (Figure 1b), then, in general, the position of the connection point (② in Figure 1b) cannot be determined uniquely.

Even worse, continuum models, which are constructed as elliptic PDEs coupled with the laws of perfect plasticity, generally do not possess a solution for strain as a function of position even when the applied body force is smoothly distributed. Instead, as it was realized first by Moreau [61], strain variable should be a time-dependent measure. This is because, in a generic scenario, the displacement variable inevitably develops discontinuities on the surfaces of codimension one inside a perfectly plastic body, and such discontinuities are incompatible with the trace theorem for Sobolev

functions, see the discussions in [21, p. 239] and [84, p. vi]. The discontinuity surfaces are called *strain localizations*, *shear bands* and *plastic slips* by various authors.

While Moreau considered a prototypical example with one spatial dimension (i.e., a rod), in order to describe strain localization in two- and three-dimensional domains the theory of the space of bounded deformations (*BD*) was developed, with major contributions by Suquet [80–83], Temam and Strang [77, 84, 85]. More recent treatments of the problems with perfect plasticity include [21, 25, 27, 31, 60]. Additionally we suggest our previous work [37] focused on the detailed comparison of discrete (such as Figure 1b) and continuum (PDE) models with perfect plasticity. Also, it should be noted that one can work around the non-uniqueness and discontinuity issues in a thin beam model by considering only small displacements orthogonal to the beam axis [50].

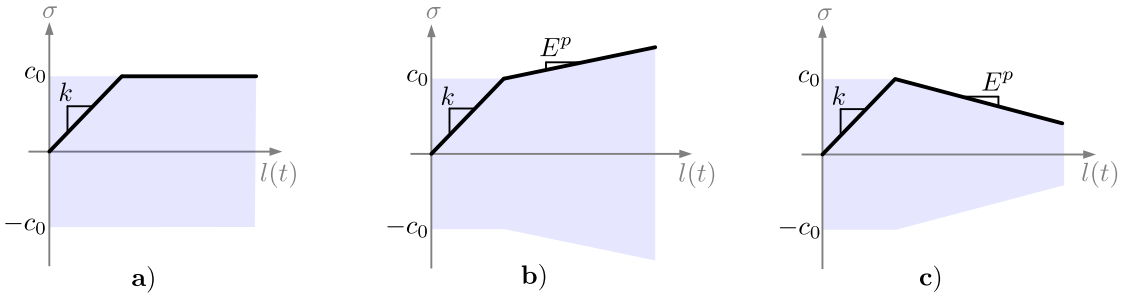

Figure 2. a) Elasticity-perfect plasticity: the stress remains constant during plastic deformation, and the set of admissible stresses (the size of the blue area along the σ axis) is fixed. b) Elasto-plasticity with hardening: during plastic deformation stress increases under imposed elongation, and the set of admissible stresses enlarges. c) Elasto-plasticity with softening: during plastic deformation stress decreases under imposed elongation, and the set of admissible stresses contracts.

1.2. Plasticity with hardening

Thus, well-posedness requires an injective stress-strain relation, and this is the case for another class of rate-independent models: plasticity with *hardening*. Hardening here means that, upon reaching the yield limit, the stress continues to increase at a slower rate $E^p < k$ along with progressive plastic deformation (see Figure 2b), and such rate E^p (called the *modulus of plasticity*) is positive, unlike the case of perfect plasticity. It is common to think of hardening as an expansion of the set of admissible stresses: in the one-dimensional spring example, instead of constraint (1.1) we have, say,

$$\sigma \in [-(c_0 + s\alpha), c_0 + s\alpha], \tag{1.2}$$

where s is another material constant to characterize plasticity, and α is a time-dependent unknown variable, usually called the *internal variable*. In the models with hardening the value of α changes during the plastic deformation, and so does the set of admissible stresses, see again Figure 2b and also see [76, Figures 1.4B and 1.6] for more details.

Plasticity with hardening is the "nicest" among the problems of our interest in the sense that the evolution of all unknown variables can be solved uniquely, and, for continuous media in particular, with values in Sobolev spaces. The well-posedness of the problem with hardening attracted many researchers in mathematics and engineering, and the literature on the topic is abundant. For proper

mathematical formulations and for proofs of existence and uniqueness of solutions for continuous elastoplastic media with hardening we refer to [65, Section 13.5] and to the monumental book [42], which is solely focused on solving this particular type of the problem. The corresponding numerical algorithms are also presented in [76]. In turn, spatially discrete models (networks of elasto-plastic springs) with hardening are the main topic of the paper [57].

1.3. Moreau's sweeping process and evolution variational inequalities

From the mathematical perspective, such mechanical problems can be posed as *evolution variational inequalities*, which were properly studied since 1970s [26] at least. In particular, the problem of plasticity with hardening and the stress problem of perfect plasticity can be expressed mathematically as a variational inequality known as a *sweeping process*, devised by Moreau about the same time [62] and [63, Secttion 5.f].

The sweeping process is an abstract problem to find a trajectory of a point X, which is subject to the one-sided constraint

$$X(t) \in C(t), \tag{1.3}$$

where $C(t)$ is a given time-dependent closed convex set, usually called the *moving set*. It can be visualized as a container, placed on top of a small object, which lies on a rough surface, so that the moving boundary of the container pushes the object upon a contact, see [59, Figure 1.2]. Naturally, (1.3) alone is not enough to specify a trajectory of X, and the sweeping process is written mathematically as the following inclusion:

$$-\dot{X}(t) \in N_{C(t)}(X(t)) \qquad \text{for a.a. } t \in [0,T], \tag{1.4}$$

where the right-hand side is the cone of outward normal (supporting) vectors to the convex set $C(t)$ at $X(t)$, defined only for (1.3) as

$$N_{C(t)}(X(t)) = \{Y : \langle Y, c - X(t)\rangle \leqslant 0 \text{ for all } c \in C(t)\}. \tag{1.5}$$

Substitute (1.5) into (1.4) to obtain the evolution variational inequality form of the problem:

$$\text{find } X(t) \in C(t) \quad \text{ such that } \quad \langle \dot{X}(t), c - X(t)\rangle \geqslant 0 \quad \text{ for all } \quad c \in C(t), \quad \text{ a.a. } \quad t \in [0,T]. \tag{1.6}$$

For a reader-friendly introduction to the theory we refer to [52, pp. 1–16], from which we will state the existence and unqueness:

Theorem 1.1. *Let $\mathcal{H}$ be a Hilbert space, and $C(t) \subset \mathcal{H}$ be a closed convex nonempty set for all $t \in [0,T]$. Let $C(t)$ be Lipschitz-continuous with respect to the Hausdorff distance, i.e., there is $L > 0$ such that*

$$d_H(C(t_1) - C(t_2)) \leqslant L|t_1 - t_2| \qquad \textit{for all } t_1, t_2 \in [0,T].$$

Then for every initial value $X(0) \in C(0)$ there exists a unique solution of the sweeping process (1.4)*, which will be Lipschitz-continuous with the same constant L.*

When the problems of elastoplasticity are expressed as a sweeping process, Theorem 1.1 yields existence and uniqueness

- of the stress solution in problems with perfect plasticity: an interested reader may compare [26, (4.20)–(4.22), p. 248] and [65, (4.16), p. 326] to (1.6), [38, (48), p. 23] and [39, (18), p. 8] to (1.4), also see [37, Section 4].

- of the solution in problems with hardening: compare [42, (8.16), p. 230] and [65, (5.11), p. 331] to (1.6).

1.4. Plasticity with softening

Finally, let us return to the example of an elasto-plastic spring and consider the case when the stress decreases along with progressive plastic deformation. This phenomenon is called *softening*, and it can be modeled as a shrinkage of the set of admissible stresses, see Figure 2c. Softening is the most difficult case in our list, as the elongation-stress (or strain-stress) relation is "worse" than non-injective — it is non-monotone.

If just two springs with softening are coupled in series (Figure 1b) then, similarly to perfect plasticity, we have multiple solutions for the position of the connection point ②. Moreover, now the stress values are not unique as well; we will verify this in Section 5, see also [17]. Written in a variational form, such a system has a non-convex energy increment with multiple isolated minima and a saddle point.

Predictably, continuous media with the strain-stress relation of the type of Figure 2c at each point of a body make an extremely challenging problem. Consider even the simplified equilibrium problem without inequalities: For a small time-step during plastic deformation a known subset of points must follow the linear yet decreasing strain-stress relation. Such a problem *will not be elliptic*, thus, no opportunity to use Lax-Milgram-type theorems [34, Section 1.1].

The non-convexity in the variational formulation also rules out the standard infinite-dimensional convex optimization [28, Section II.1, pp. 34–36]. Analytic results on a one-dimensional continuum in the variational formulation can be found in [11, 56]. For 2- and 3-dimensional bodies there exists a rather difficult variational theory by Dal Maso et al. [22, 23]. They have demonstrated the existence of a solution in the space of compatible systems of generalized Young measures, confirmed non-uniqueness of solutions [23, Remark 5.2] and the presence of strain localizations [22, Section 8.2] in their formulation.

On the other hand, plasticity with softening was researched extensively in mechanical and civil engineering. There it was observed that strain localization due to softening is the initial phase of *ductile fracture* [8,36,69]. In other words, ductile fracture follows plastic deformation, and this makes it different from brittle fracture, which may occur abruptly without any preceding plastic deformation [14, Chapter 13]. An interested reader may find mathematical analysis of brittle fracture models based on the classical Griffith criterion in numerous works, e.g., [24, 32, 47]. However, they do not cover the failure of a ductile material, as one needs a model of elasto-plasticity with softening to correctly account for structural effects influencing the gradual degradation of the material.

We will not attempt to provide a comprehensive overview of the great amount of engineering publications on the topic, and only mention a few of ample contributions by Bažant [8, 69], Jirásek [44, 45] and de Borst [9, 10, 73], where the reader can find related discussions. Notably, there is a fundamental issue of severe mesh-dependence in numerical simulations due to the lack of ellipticity of the problem. Finite element approximations develop strain localizations to a layer of single elements

and such dependence on the size of elements invalidates the objectivity of the models. For this reason, much of the literature is devoted to non-local modifications of the constitutive law that limit strain localizations.

Because of such difficulties, we will not consider continuum media in this text, and focus instead of the discrete models, such as toy models of Figure 1 and networks of springs (also known as Lattice Spring Models (LSMs), or, informally, "trusses"), see Figure 3. Such spring models have already been used to model fracture [18,58] and our work is a step towards a rigorous mathematical theory for them.

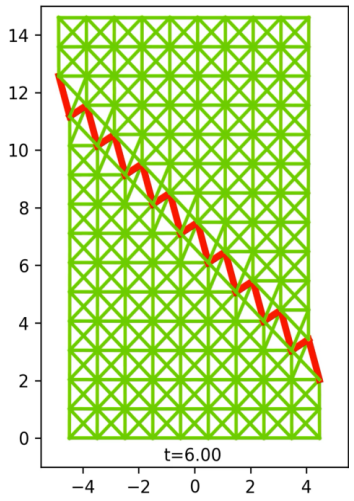

Figure 3. A network of springs with softening developed a shear band. Such numerical examples will be presented in Section 6.

We extend the sweeping process approach of [38] and formulate the elastoplasticity problem for discrete media in terms of stress and internal variable ("the dual problem" according to [42]) in such a way it includes not only perfect plasticity, but also hardening and, most importantly, softening. However, this will inevitably require a more general formalism than the "classical" sweeping process (1.4).

1.5. State-dependent sweeping process

As we mentioned in the beginning of the previous Section 1.4, in the case of softening the evolution of stresses may not be unique even in such a simple model as Figure 1b. This is clearly incompatible with the uniqueness of the solution stated in Theorem 1.1 and excludes any expectation that the problem with softening can be converted to the form (1.4).

Instead, we will adopt a richer framework of the *state-dependent sweeping process*, i.e., the modification of (1.4) with the moving set C not just being a prescribed function of t, but also depending on the state variable X:

$$-\dot{X} \in N_{C(t,X)}(X). \tag{1.7}$$

This type of problem was investigated by Kunze et al. [53], see also [52, Section 3.3, pp. 23–29], from where we adopt the counterpart of Theorem 1.1 for the state-dependent sweeping process in finite dimensions:

Theorem 1.2. *[52, Theorem 6, p. 25], [53, Theorem 3.3, p. 184] Let E be a Euclidean space, and $C(t, X) \subset E$ be a closed convex nonempty set for all $t \in [0, T], X \in E$. Let $C(t, X)$ have Lipschitz-continuous dependence on t and X with respect to the Hausdorff distance, i.e., there are $L_1, L_2 > 0$ such that*

$$d_H(C(t_1, X_1) - C(t_2, X_2)) \leqslant L_1|t_1 - t_2| + L_2\|X_1 - X_2\| \qquad \text{for all } t_1, t_2 \in [0, T],\ X_1, X_2 \in E. \tag{1.8}$$

If

$$L_2 < 1 \tag{1.9}$$

then for every initial value $X(0)$, compatible in the sense that $X(0) \in C(0, X(0))$, there exists at least one solution of the state-dependent sweeping process (1.7)*.*

Conditions (1.8)-(1.9) are nowadays the standard requirement for the existence of a solution in this type of problems, generalized to many further modifications of the problem (1.7) (perturbed by a vector field [41], with a non-convex prox-regular moving set [16, 48], with a lower regularity in time [46, 49, 74], etc.). But condition (1.9) remains essential for the existence, as for $L_2 \geqslant 1$ there are simple counterexamples with no solutions (see the references cited for Theorem 1.2).

Moreover, the uniqueness of a solution to (1.7) is not guaranteed at all regardless of the value of L_2, see the discussion [13, p. 112]. It is also shown there that uniqueness can be achieved if the set C has a sufficiently smooth boundary. But in the problems of our interest neither uniqueness of a solution, nor a smooth boundary of C will be present.

As the central result of this text, the problem of quasi-static evolution of a network of springs (including softening, hardening, and perfectly plastic springs) will be converted to the initial value problem governed by a state-dependent sweeping process (1.7) (Theorem 4.1) and solved numerically. This way, all of the plastic properties of the springs and the way they are connected will be encoded into the set $C(t, X)$.

To find a numerical solution to the problem (1.7) we use the *implicit catch-up algorithm* of [53]. In the algorithm we must take a partition of the time-domain $[0, T]$:

$$0 = t_0 < \cdots < t_{i-1} < t_i < \ldots t_k = T, \quad i \in \overline{1, k}$$

and for each time-step we must find $X_{i+1} \in E$, such that

$$X_i - X_{i+1} \in N_{C(t_{i+1}, X_{i+1})}(X_{i+1}), \tag{1.10}$$

which is equivalent to the fixed-point problem, involving a projection onto a closed convex set:

$$X_{i+1} = \operatorname{proj}(X_i, C(t_{i+1}, X_{i+1})). \tag{1.11}$$

To find such fixed points we will numerically run the iterations of the map

$$\tilde{X} \mapsto \operatorname{proj}\left(X_i, C\left(t_{i+1}, \tilde{X}\right)\right). \tag{1.12}$$

This method works in practice, yet it raises the questions not only about the *existence* of the fixed points, but also about their *stability* as equilibria of the discrete dynamical system, defined by the map (1.12). And, although the conditions of Theorem 1.2 yield the existence (see [53, Lemma 2.1,

p. 182]), we will see that they only cover the "nicest" case of hardening. Furthermore, the stability of such dynamical systems is largely unexplored.

Another way to look at the problem (1.10) is to convert it to the equivalent form of a *quasi-variational inequality* (see [4, Section 11, pp. 237–261] and references therein), for which there are more numerical methods available, e.g., in [29, 30, 68].

Our particular line of research on modeling softening as a state-dependent sweeping process was initiated in 1990s by Brokate and Studt, but it was interrupted at the time. One can still find a trace of Studt's PhD thesis (see [53]), which is confirmed to be never finished and never published. The work was continued by Brokate et al. [13] and Schnabel [75], with their results, aimed at a particular type of softening, known as Gurson's model [40, 66, 86]. Brokate et al. proved uniqueness of solutions, yet they considered single-element ("zero-dimensional") models. In recent work, Bauer et al. [6] employ a non-convex prox-regular state-dependent sweeping process to model the plastic-like behavior of a railway foundation and prove both existence and uniqueness; the constitutive relation there is similar to nonlinear hardening. In the current work, we demonstrate how coupling of just two elements (Figure 1b with softening leads to non-uniqueness.

The paper is organized as follows:

- In the next Section 2 we briefly remind the reader a few basic definitions and properties, which we will use later.
- In Section 3 we derive the state-dependent sweeping process for a single spring and show that, with different values of parameters we can reproduce all three types of plasticity of Figure 2. Such state-dependent sweeping process is two-dimensional, as it represents the joint evolution of stress and the internal variable in the toy model of Figure 1a.
- In Section 4 we connect m such springs into a lattice according to a given graph and derive the state-dependent sweeping process in $2m$ dimensions to model the evolution of the entire lattice. The dimension $2m$ can be reduced to an extent depending on the underlying graph of the lattice, and this is important for speeding up the numerical algorithm.
- In Section 5 we focus on a specific example of the lattice, the toy model of Figure 1b. We analytically show non-uniqueness of solutions in the corresponding state-dependent sweeping process, which agrees with [17], where the same spring model is studied. Notably, for this particular state-dependent sweeping process, we can directly observe how the implicit catch-up algorithm can find unique and non-unique solutions. We also visualize the moving set $C(t, X)$ to understand how such multiple solution are possible in the case of softening.
- In Section 6 we provide several examples of more complex LSMs (similar to Figure 3) to compare the cases of hardening, perfect plasticity and softening. We observe the formation of shear bands and non-uniqueness of solutions, especially in the latter case.
- Finally, Section 7 contains a concluding summary and a discussion on open questions.

2. Notation and technical preliminaries

By 0_n we denote the zero vector in $\mathbb{R}^n$ and $I_{n\times n}$ is the $n \times n$ identity matrix. We use the following notation for the normal cone in a subspace of $\mathbb{R}^n$ (see [7, p. 125], [52, p. 3], [71, p. 15] for a general

definition of the normal cone $N_C(x)$ a Hilbert space):

Definition 2.1. Given a vector space $E \subset \mathbb{R}^n$, for an $n \times n$ symmetric positive definite matrix S we can define an inner product on E

$$(x, y) \mapsto \langle x, y\rangle_S := x^\top S y \qquad \text{for any } x, y \in E. \tag{2.1}$$

Now, for a closed convex nonempty set $C \subset E$ and a point $x \in E$ we define the *outward normal cone to C at x in sense of inner product $\langle\cdot,\cdot\rangle_S$* as

$$N_C^S(x) := \{y \in E : y^\top S(c - x) \leqslant 0 \text{ for all } c \in C\}.$$

If $S = I$ we simply write $N_C(x)$.

Proposition 2.1. *In the setting of Definition 2.1 it follows from the definition that for any $y \in E$*

$$N_C^S(x + y) = N_{C-y}^S(x), \tag{2.2}$$

$$S\, N_C(x) = N_C^{S^{-1}}(x). \tag{2.3}$$

$$y - x \in N_C^S(x) \qquad \Longleftrightarrow \qquad x = \operatorname{proj}^S(y, C), \tag{2.4}$$

where

$$\operatorname{proj}^S(y, C) := \arg\min_{c \in C} (y - c)^\top S\, (y - c).$$

The following fact may appear trivial, however, we verify it for the sake of completeness of the proofs.

Lemma 2.1. *Let E be an Euclidean space with the inner product $\langle\cdot,\cdot\rangle_E$. Let us be given a family of m convex polytopes C_i, $i \in \mathbb{N}$. Consider the space E^m with the inner product*

$$(x_i)_{i\in\overline{1,m}},\ (y_i)_{i\in\overline{1,m}} \mapsto \left\langle (x_i)_{i\in\overline{1,m}}, (y_i)_{i\in\overline{1,m}} \right\rangle_{E^m} = \sum_{i=1}^m \langle x_i, y_i\rangle_E$$

and the set

$$C := \left\{(x_i)_{i\in\overline{1,m}} \in E^m : x_i \in C_i \text{ for all } i \in \overline{1,m}\right\} = C_1 \times C_2 \times \cdots \times C_m.$$

Then for any $x^* = (x_i^*)_{i\in\overline{1,m}} \in C$

$$N_C(x^*) = N_{C_1}(x_1^*) \times N_{C_2}(x_2^*) \times \cdots \times N_{C_m}(x_m^*). \tag{2.5}$$

Proof. For each $i \in \overline{1,m}$, let

$$\mathrm{C}_i := \left\{(x_j)_{j\in\overline{1,m}} \in E^m : x_i \in C_i\right\} = E \times \cdots \times E \times C_i \times E \times \cdots \times E.$$

From the definition of the normal cone we can derive that

$$N_{\mathrm{C}_i}(x^*) = \{0\} \times \cdots \times \{0\} \times N_{C_i}(x_i^*) \times \{0\} \times \cdots \times \{0\}. \tag{2.6}$$

Observe that $C = \bigcap_{i=1}^m \mathrm{C}_i$, therefore, by the additivity of the normal cones for polyhedra we have

$$N_C(x^*) = \sum_{i=1}^m N_{\mathrm{C}_i}(x^*),$$

from which (2.5) follows because of (2.6). □

3. Single spring element: constitutive equations, the corresponding sweeping process and its analysis

3.1. An elasto-plastic spring element with the state-dependent normality rule

We begin with a mathematical description of a single spring, so that in the later sections many such springs could be assembled to a lattice. At each moment of time the state of the spring is characterized by the following scalar variables: the *total elongation* x, the *elastic elongation* ε, the *plastic elongation* p, the *stress* σ and the *damage variable* a. The latter is also called the *internal variable*. The usual constitutive laws are:

$$\text{additive decomposition:} \qquad x = \varepsilon + p, \tag{3.1}$$

$$\text{Hooke's law:} \qquad \sigma = k\varepsilon, \tag{3.2}$$

where parameter $k > 0$ is the stiffness of the spring. We assume the following plastic flow rule to hold for a.a. t from a given time-interval $[0, T]$:

$$\frac{d}{dt}\begin{pmatrix} p \\ -a \end{pmatrix} \in N_{\mathrm{C}+\begin{pmatrix} 0 \\ ha \end{pmatrix}}\begin{pmatrix} \sigma \\ a \end{pmatrix}. \tag{3.3}$$

In the current text we focus on the linear case and put C as

$$\mathrm{C} := \left\{ \begin{pmatrix} \sigma \\ \alpha \end{pmatrix} \in \mathbb{R}^2 : -(c_0 + s\alpha) \leqslant \sigma \leqslant c_0 + s\alpha \right\}. \tag{3.4}$$

We use α to distinguish the dummy variable in the definition of C from the actual state variable a (they also differ by a translation on ha, so that they have different meanings). The corresponding state-dependent set in (3.3) is illustrated in Figure 4a. Here we assume that $h \in \mathbb{R}$, $s \geqslant 0$ and $c_0 > 0$ are the parameters of the spring which describe its behavior in the plastic regime. We call h, s and c_0 the *coefficient of state-dependent feedback*, the *geometric slope* and the *initial yield stress* respectively.

The admissible stresses of the spring are defined via the "horizontal" section of Figure 4a at a specified value of a:

$$\left\{ \begin{pmatrix} \sigma \\ a \end{pmatrix} : \sigma \in \mathbb{R} \right\} \cap \left(\mathrm{C} + \begin{pmatrix} 0 \\ ha \end{pmatrix} \right),$$

cf. [76, Figure 1.6], i.e., with C given as (3.4) we have the set of admissible stresses

$$\sigma \in [-(c_0 + s(1-h)a,\ c_0 + s(1-h)a].$$

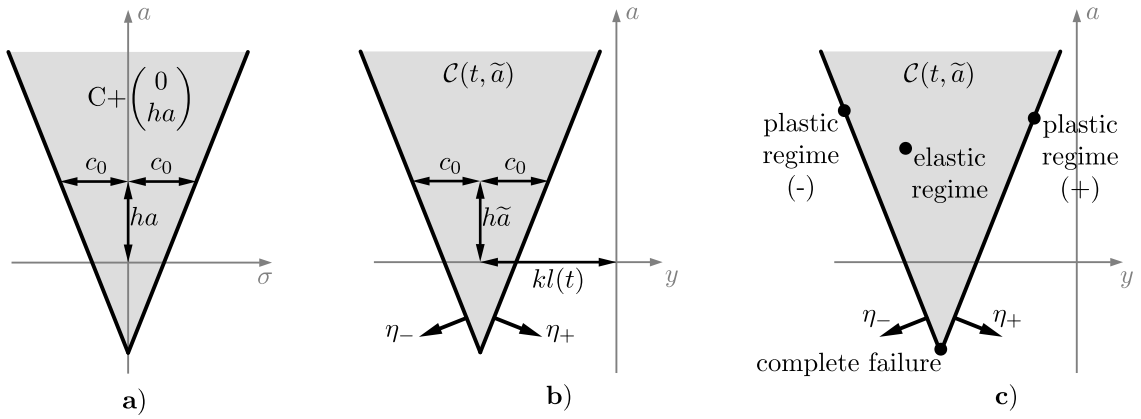

Figure 4. a) Set $\mathrm{C} + \begin{pmatrix} 0 \\ ha \end{pmatrix}$ in plastic flow rule (3.3) and (3.4). b) The corresponding moving set (3.9) in the state-dependent sweeping process (3.8). c) Four possible regimes of the single spring model.

3.2. A state-dependent sweeping process for a single spring

Before we proceed to the construction of lattices we shall explain the behavior of a single spring, described by (3.1)–(3.4). To such a spring we apply a displacement loading (see Figure 1a)

$$x = l(t). \tag{3.5}$$

From (3.1), (3.2) and (3.5) we get that

$$kp = kl(t) - \sigma.$$

Then it follows from (2.3) and (3.3) that

$$\frac{d}{dt}\begin{pmatrix} kl(t) - \sigma \\ -a \end{pmatrix} = \frac{d}{dt}\begin{pmatrix} kp \\ -a \end{pmatrix} = \mathbb{K}\,\frac{d}{dt}\begin{pmatrix} p \\ -a \end{pmatrix} \in \mathbb{K}\,N_{\mathrm{C}+\begin{pmatrix} 0 \\ ha \end{pmatrix}}\begin{pmatrix} \sigma \\ a \end{pmatrix} = N^{\mathbb{K}^{-1}}_{\mathrm{C}+\begin{pmatrix} 0 \\ ha \end{pmatrix}}\begin{pmatrix} \sigma \\ a \end{pmatrix},$$

where

$$\mathbb{K} = \begin{pmatrix} k & 0 \\ 0 & 1 \end{pmatrix}.$$

Denote

$$y := \sigma - kl(t) \tag{3.6}$$

and deduce that the single spring model (3.1)–(3.5) is equivalent to the following inclusion in $\mathbb{R}^2$:

$$-\frac{d}{dt}\begin{pmatrix} y \\ a \end{pmatrix} \in N^{\mathbb{K}^{-1}}_{\mathrm{C}+\begin{pmatrix} -kl(t) \\ ha \end{pmatrix}}\begin{pmatrix} y \\ a \end{pmatrix}. \tag{3.7}$$

Inclusion (3.7) is a state-dependent sweeping process.

3.3. Analysis of the plastic behavior of the single spring

Now we can analyze the behavior of the single spring by looking at the process (3.7). For convenience, we first rewrite it in the compact form:

$$-\frac{d}{dt}\begin{pmatrix} y \\ a \end{pmatrix} \in N^{\mathbb{K}^{-1}}_{C(t,a)}\begin{pmatrix} y \\ a \end{pmatrix}. \tag{3.8}$$

The following is the definition of state-dependent moving set $C(t,a)$, in which we must distinguish between the parameter $\tilde{a}$ and the dummy variables a, α.

$$\begin{aligned} C(t,\tilde{a}) &:= \left\{ \begin{pmatrix} \sigma - kl(t) \\ \alpha + h\tilde{a} \end{pmatrix} : \begin{pmatrix} \sigma \\ \alpha \end{pmatrix} \in \mathbb{R}^2,\ -(c_0 + s\alpha) \leqslant \sigma \leqslant c_0 + s\alpha \right\} \\ &= \left\{ \begin{pmatrix} y \\ a \end{pmatrix} \in \mathbb{R}^2 : -(c_0 + s(a - h\tilde{a})) \leqslant y + kl(t) \leqslant c_0 + s(a - h\tilde{a}) \right\} \\ &= \left\{ \begin{pmatrix} y \\ a \end{pmatrix} \in \mathbb{R}^2 : \begin{array}{c} -(y + kl(t)) - s(a - h\tilde{a}) \leqslant c_0, \\ (y + kl(t)) - s(a - h\tilde{a}) \leqslant c_0 \end{array} \right\} \\ &= \left\{ \begin{pmatrix} y \\ a \end{pmatrix} \in \mathbb{R}^2 : \begin{array}{c} \eta_-^\top \mathbb{K}^{-1} \begin{pmatrix} y + kl(t) \\ a - h\tilde{a} \end{pmatrix} \leqslant c_0, \\ \eta_+^\top \mathbb{K}^{-1} \begin{pmatrix} y + kl(t) \\ a - h\tilde{a} \end{pmatrix} \leqslant c_0 \end{array} \right\}, \end{aligned} \tag{3.9}$$

where

$$\eta_- := \begin{pmatrix} -k \\ -s \end{pmatrix}, \qquad \eta_+ := \begin{pmatrix} k \\ -s \end{pmatrix}, \tag{3.10}$$

see Figure 4b. It is clear, that the solution of such sweeping process can be in one of the four following regimes, see also Figure 4c:

- *Elastic regime*, when $(y,a) \in \operatorname{int} C(t,a)$;
- The *plastic regime* of maximal stress, when the constraint with the normal η_+ is active;
- The *plastic regime* of minimal stress, when the constraint with the normal η_- is active;
- The *state of complete failure*, when both constraints are active. Such state means, that the current set of admissible stresses is degenerate, i.e., it is the singleton-zero set $\{0\}$.

In the elastic regime formulas (3.6) and (3.7) simply mean that

$$\dot{y}(t) = 0, \qquad \dot{a}(t) = 0, \qquad \sigma(t) = \sigma(0) + kl(t).$$

We explicitly solve the evolution in the plastic regimes over the intervals of monotonic load $l(t)$ in the following proposition, where we mean the signs $\pm$ and $\mp$ to be, respectively, $+$ and $-$, or $-$ and $+$ to combine both cases in one statement.

Proposition 3.1. *Let*

$$k^{-1}s^2(1-h) > -1. \tag{3.11}$$

If y_0, a_0 and t_0 are such that the constraint with $\eta_\pm$ is active, i.e.,

$$\eta_\pm^\top \mathbb{K}^{-1} \begin{pmatrix} y_0 + kl(t_0) \\ (1-h)a_0 \end{pmatrix} = c_0 \tag{3.12}$$

and $\pm\dot{l}(t) \geqslant 0$ for $t \geqslant t_0$, then

$$\begin{pmatrix} y(t) \\ a(t) \end{pmatrix} := \begin{pmatrix} y_0 \\ a_0 \end{pmatrix} \mp \frac{1}{1 + k^{-1}s^2(1-h)} \eta_\pm l(t) \tag{3.13}$$

is a solution of the state-dependent sweeping process (3.8)–(3.10) *as long as the other constraint remains inactive, i.e.*

$$\eta_\mp^\top \mathbb{K}^{-1} \begin{pmatrix} y + kl(t) \\ (1-h)a \end{pmatrix} < c_0. \tag{3.14}$$

Proof. We need to find a non-negative $\lambda(t)$ such that

$$-\begin{pmatrix} \dot{y}(t) \\ \dot{a}(t) \end{pmatrix} = \lambda(t)\, \eta_\pm \tag{3.15}$$

and

$$\eta_\pm^\top \mathbb{K}^{-1} \begin{pmatrix} \dot{y}(t) + k\dot{l}(t) \\ (1-h)\dot{a}(t) \end{pmatrix} = 0. \tag{3.16}$$

Finding such λ will be sufficient to guarantee that

$$\begin{pmatrix} y \\ a \end{pmatrix} = \begin{pmatrix} y_0 \\ a_0 \end{pmatrix} + \int_{t_0}^{t} \begin{pmatrix} \dot{y}(\tau) \\ \dot{a}(\tau) \end{pmatrix} d\tau$$

is a solution, because (3.12) and (3.16) imply that the constraint with $\eta_\pm$ is active for all $t \geqslant t_0$, so that $(y, a) \in C(t, a)$ as long as the constraint with $\eta_\mp$ is not active, while (3.15) means that the inclusion (3.8) holds.

From (3.15) we obtain

$$\begin{pmatrix} \dot{y}(t) \\ \dot{a}(t) \end{pmatrix} = \begin{pmatrix} \mp k\lambda(t) \\ s\lambda(t) \end{pmatrix},$$

then we plug it into (3.16):

$$\begin{pmatrix} \pm k \\ -s \end{pmatrix}^\top \begin{pmatrix} k^{-1} & 0 \\ 0 & 1 \end{pmatrix} \begin{pmatrix} \mp\lambda(t)k + k\dot{l}(t) \\ (1-h)s\lambda(t) \end{pmatrix} = 0,$$

$$-k\lambda(t) \pm k\dot{l}(t) - (1-h)s^2\lambda(t) = 0,$$

$$\lambda(t) = \pm\frac{k\dot{l}(t)}{k + (1-h)s^2} = \pm\frac{1}{1 + k^{-1}s^2(1-h)}\, \dot{l}(t).$$

Hence

$$\begin{pmatrix} \dot{y}(t) \\ \dot{a}(t) \end{pmatrix} = \mp\frac{1}{1 + k^{-1}s^2(1-h)}\, \dot{l}(t)\eta_\pm.$$

Observe that (3.11) and $\pm\dot{l}(t) \geqslant 0$ guarantee that $\lambda(t) \geqslant 0$. Thus, we have shown that (3.13) is indeed a solution of (3.8)–(3.10) under the conditions listed. □

Corollary 3.1. *Under the conditions of Proposition 3.1 we have the evolution of the stress as the following:*

$$\begin{aligned}\sigma(t) = y(t) + kl(t) &= y_0 - \frac{k}{1 + k^{-1}s^2(1-h)}l(t) + kl(t)\\ &= \sigma_0 - kl(t_0) + \frac{s^2(1-h)}{1 + k^{-1}s^2(1-h)}l(t).\end{aligned}$$

These computations allow us to characterize the behavior of the spring as follows:

Observation 3.1. Constitutive Eqs (3.1)–(3.4) describe a spring with elasticity modulus k in the elastic regime. In the plastic regimes, we can have different types of plasticity, depending on the parameters:

- If $h = 1$ (Figure 5a) or $s = 0$ (Figure 5b) then it is the case of *perfect plasticity* (Figure 5c).

- If $s^2(1-h) > 0$ then it is the case of linear isotropic *hardening* (Figure 5d,e) with *plasticity modulus*

$$E^p = \frac{s^2(1-h)}{1 + k^{-1}s^2(1-h)}. \tag{3.17}$$

- If $0 > k^{-1}s^2(1-h) > -1$ then it is linear isotropic *softening* with plasticity modulus E^p (Figure 5f,g).

Notice that if $k^{-1}s^2(1-h) \to -1$ from above then we have $E^p \to -\infty$, so we exclude the situation of $k^{-1}s^2(1-h) \geqslant -1$ from further consideration in this paper. Furthermore, if $s^2(1-h) \to +\infty$ with k fixed, then $E^p \to k$ from below, i.e., the limit of hardening moduli is elastic stiffness of the spring, see Figure 6.

If one is interested in modeling perfect plasticity and hardening phenomena (but not softening), it is possible to construct a sweeping process analogous to (3.8) with the moving set depending on t only, see the references at the end of Section 1.3. In this paper our main interest is softening, however, we do not exclude the other two cases, so that we are able to compare between them. Also, we preserve the opportunity to include perfectly plastic and hardening springs in the same lattice with softening springs.

Remark 3.1. If a spring with linear softening plasticity reaches a state where both constraints of (3.9) are active at (y, a) (see, e.g., the position at $t = t_4$ on Figure 7a,b), then it means complete failure of the spring, as for a further change of the load the solution is not continuable. This could be viewed as separation of the material at the endpoints of the spring due to ductile fracture.

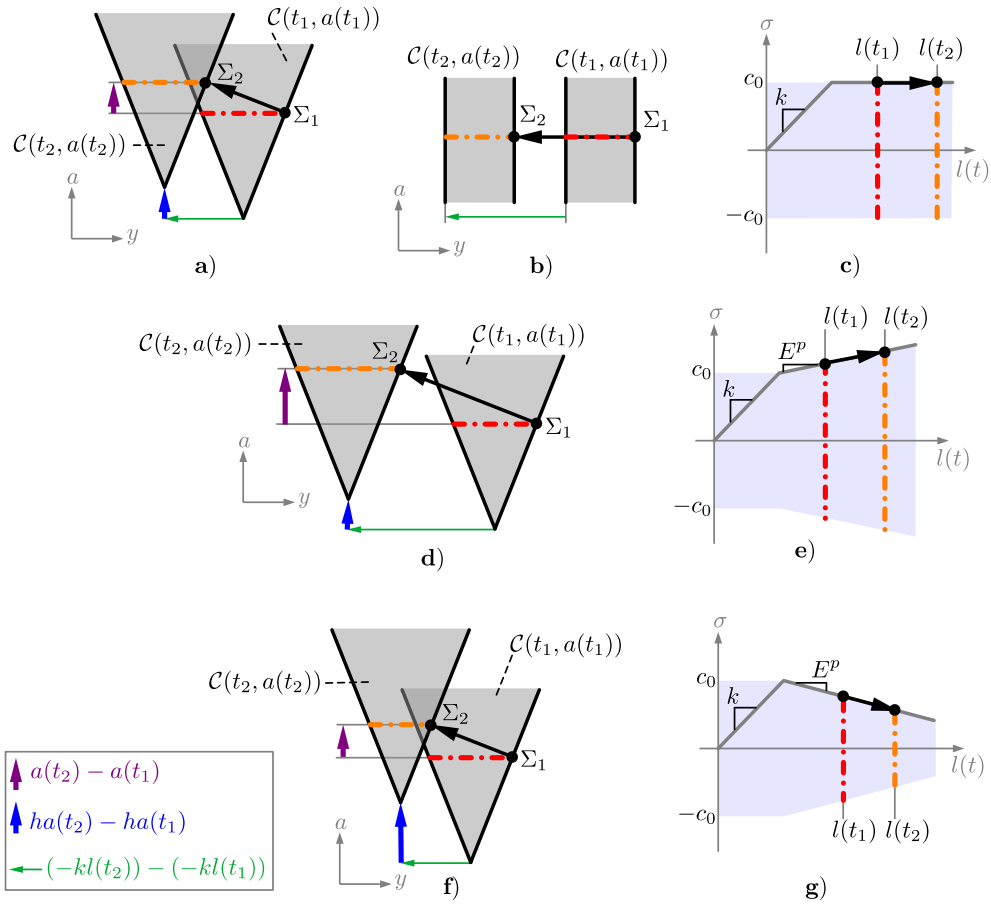

Figure 5. Evolution in the state-dependent sweeping process (3.8)-(3.9) and the corresponding displacement-stress plots for different types of linear isotropic plasticity of an isolated spring, Figure 1a under monotonically increasing displacement load $l(t)$. Here $t_1 < t_2, \Sigma_1 := (y(t_1), a(t_1)), \Sigma_2 := (y(t_2), a(t_2))$. a) $h = 1$ leads to perfect plasticity, because $a(t_2) - a(t_1)$ (purple) equals to the term $ha(t_2) - ha(t_1)$ of state-dependent translation (blue) of the moving set C, which leads to the set of admissible stresses being constant in time. Indeed, observe, that the set of admissible stresses at t_1 (red) is the same as at t_2 (orange). b) $s = 0$ leads to perfect plasticity as well, because damage variable a cannot change, and set of admissible stresses remains the same between t_1 (red) and t_2 (orange). c) Displacement-stress plot illustrates the case of perfect plasticity characterized by the set of admissible stresses remaining the same between t_1 (red) and t_2 (orange). d) Parameters $s > 0$ and $h < 1$ lead to hardening: notice how the term $ha(t_2) - ha(t_1)$ of state-dependent translation (blue) of the moving set is smaller than the change $a(t_2) - a(t_1)$ (purple) of the state variable. Because of this the set of admissible stresses expands between t_1 (red) and t_2 (orange). e) Displacement-stress plot for hardening, which is happening when the set of admissible stresses expands between t_1 (red) and t_2 (orange). f) Parameters $s > 0$ and $h > 1$ lead to softening: the term $ha(t_2) - ha(t_1)$ of state-dependent translation (blue) of the moving set is greater than the change $a(t_2) - a(t_1)$ (purple) of the state variable. This results in the set of admissible stresses shrinking between t_1 (red) and t_2 (orange). g) Displacement-stress plot for softening, which is happening when the set of admissible stresses shrinks between t_1 (red) and t_2 (orange).

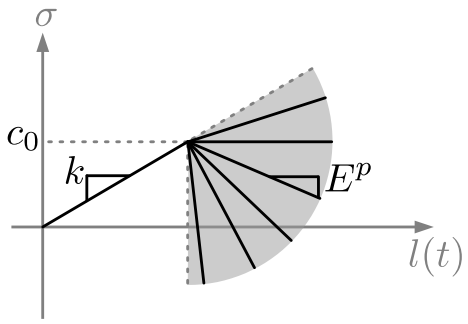

Figure 6. The range $(-\infty, k)$ of plasticity moduli E^p which we consider in this paper, cf. [76, p. 88]. A plasticity modulus E^p is computed by (3.17) from the parameters in the state-dependent plastic flow rule (3.3)-(3.4) and in Hooke's law (3.2).

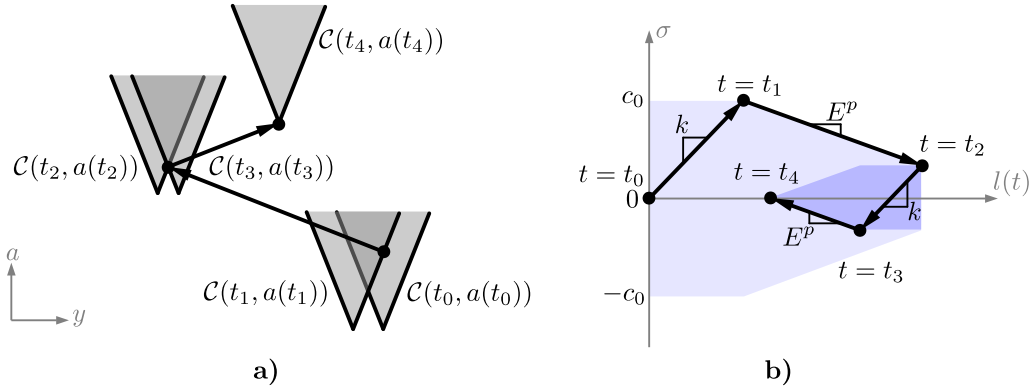

Figure 7. Modeling of the evolution of an elasto-plastic spring with linear isotropic softening, starting from the relaxed initial state. At $t = t_0$ we start from the stress-free state and apply increasing displacement loading $l(t)$. At $t = t_1$ the spring changes from elastic to plastic regime. At $t = t_2$ the derivative of the applied displacement load is reversed ($l(t)$ is now decreasing), which makes the spring to return to the elastic regime and undergo *elastic unloading* [42, Section 3.1]. At $t = t_3$ the lower elastic threshold is attained, so the spring switches to the plastic mode again. Notice that the spring has reduced set of admissible stresses compared to t_1, and this applies to both upper and lower thresholds (isotropic softening). At $t = t_4$ the spring reaches a point of complete failure, because its set of admissible stresses had reduced to $\{0\}$, and the solution cannot be continued further. a) A sketch of the evolution in the state-dependent sweeping process (3.8). Note, that during the elastic phases the solution of the sweeping process is in the interior of the moving set and remains at rest. b) The corresponding displacement–stress plot. The size of the blue area along the vertical axis indicates the set of admissible stresses for the corresponding $l(t)$.

4. Lattice Spring Model and the corresponding state-dependent sweeping process

Since we have understood the behavior of a single spring in the model (3.1)–(3.4), we can connect together m such springs to form a lattice. It is important to note that we will not not alter the constitutive laws of individual springs, but merely couple the springs at the nodes of the lattice and write the entire

problem in a vector form. Therefore, each spring in the lattice still behaves according to the analysis in the previous Section 3, and Observation 3.1 in particular.

A lattice is described by a given graph with incidence matrix Q and given reference positions of the vertices ξ_0. First, we write the system of governing equations of the entire lattice and then convert it to a state-dependent sweeping process.

4.1. The system of equations for a lattice of connected springs

This section mostly repeats the construction of [38, Section 3], where the reader can find additional details and discussions on the mechanics of the lattices in general, rather then on the question arising from softening and state-dependence.

4.1.1. Constitutive laws in a vector form

We collect the variables of individual springs into vectors, so the state of the entire lattice is described by the unknown time-dependent variables $x, \varepsilon, p, \sigma, a \in \mathbb{R}^m$ with the same meaning of their individual components as in Section 3.1. Clearly, by collecting the Eqs (3.1) and (3.2) of the individual components to vector forms we get

$$x = \varepsilon + p, \tag{LSM1}$$

$$\sigma = K\varepsilon, \tag{LSM2}$$

where K is the following diagonal matrix with positive diagonal elements:

$$K = \operatorname{diag}(k_i)_{i\in\overline{1,m}}.$$

Also, by using Lemma 2.1 with $E = \mathbb{R}^2$ and rearranging the order of components, we observe that (3.3) holds for all $i \in \overline{1,m}$ if and only if

$$\frac{d}{dt}\begin{pmatrix} p \\ -a \end{pmatrix} \in N_{\mathrm{C}+\begin{pmatrix} 0 \\ Ha \end{pmatrix}}\begin{pmatrix} \sigma \\ a \end{pmatrix}, \tag{LSM3}$$

where H is the following diagonal matrix:

$$H = \operatorname{diag}(h_i)_{i\in\overline{1,m}},$$

and C is given as

$$\mathrm{C} = \left\{\begin{pmatrix} \sigma \\ \alpha \end{pmatrix} \in \mathbb{R}^{2m} : -(c_{0,i} + s_i\alpha_i) \leqslant \sigma_i \leqslant c_{0,i} + s_i\alpha_i \text{ for all } i \in \overline{1,m}\right\}. \tag{4.1}$$

We can rewrite the state dependent set in (LSM3) as the following (again, we distinguish the parameter variable $\tilde{a}$ from dummy variables a and α)

$$\begin{aligned}
\mathrm{C} + \begin{pmatrix} 0 \\ H\tilde{a} \end{pmatrix} &= \left\{\begin{pmatrix} \sigma \\ \alpha + H\tilde{a} \end{pmatrix} : \begin{pmatrix} \sigma \\ \alpha \end{pmatrix} \in \mathbb{R}^{2m}, -(c_{0,i} + s_i\alpha_i) \leqslant \sigma_i \leqslant c_{0,i} + s_i\alpha_i \text{ for all } i \in \overline{1,m}\right\} \\
&= \left\{\begin{pmatrix} \sigma \\ a \end{pmatrix} \in \mathbb{R}^{2m} : -(c_{0,i} + s_i(a_i - h_i\tilde{a}_i)) \leqslant \sigma_i \leqslant c_{0,i} + s_i(a_i - h_i\tilde{a}_i) \text{ for all } i \in \overline{1,m}\right\} \\
&= \left\{\begin{pmatrix} \sigma \\ a \end{pmatrix} \in \mathbb{R}^{2m} : \begin{matrix} -\sigma_i - s_i(a_i - h_i\tilde{a}_i) \leqslant c_{0,i} \\ \sigma_i - s_i(a_i - h_i\tilde{a}_i) \leqslant c_{0,i} \end{matrix} \text{ for all } i \in \overline{1,m}\right\}.
\end{aligned} \tag{4.2}$$

Remark 4.1. We only consider $s_i \geqslant 0$, $i \in \overline{1,m}$, and this makes each component a_i a non-decreasing function. Indeed, for each value of parameter $\tilde{a}$ set (4.2) is a convex polytope with its normal cone

$$N_{\mathrm{C+}\begin{pmatrix} 0 \\ H\tilde{a} \end{pmatrix}} \begin{pmatrix} \sigma \\ a \end{pmatrix} = \operatorname{cone}\left\{ \left\{ \begin{pmatrix} -e_i \\ -s_i e_i \end{pmatrix} : i \in \overline{1,m} : \begin{pmatrix} -e_i \\ -s_i e_i \end{pmatrix}^{\top} \begin{pmatrix} \sigma \\ a - H\tilde{a} \end{pmatrix} = c_{0,i} \right\} \right.$$
$$\left. \cup \left\{ \begin{pmatrix} e_i \\ -s_i e_i \end{pmatrix} : i \in \overline{1,m} : \begin{pmatrix} e_i \\ -s_i e_i \end{pmatrix}^{\top} \begin{pmatrix} \sigma \\ a - H\tilde{a} \end{pmatrix} = c_{0,i} \right\} \right\}, \tag{4.3}$$

where by $e_i \in \mathbb{R}^m$ we denote the i-th vector of the standard basis. Therefore, it follows from (LSM3) that

$$-\dot{a}_i = -s_i \lambda_i \text{ for some } \lambda_i \geqslant 0,$$

and

$$\dot{a}_i \geqslant 0 \tag{4.4}$$

for a.a. $t \in [0,T]$.

Remark 4.2. We can explicitly compute the state of complete failure we mentioned in Remark 3.1. Observe that if for some $\begin{pmatrix} \sigma \\ a \end{pmatrix} \in \mathbb{R}^{2m}$ and some $i \in \overline{1,m}$ we simultaneously have both constraints in (4.2) active for $a = \tilde{a}$, i.e.,

$$\begin{aligned} -\sigma_i - s_i(1-h_i)a_i &= c_{0,i}, \\ \sigma_i - s_i(1-h_i)a_i &= c_{0,i}, \end{aligned} \tag{4.5}$$

then it necessarily means that

$$a_i = -\frac{c_{0,i}}{s_i(1-h_i)}, \qquad \sigma_i = 0,$$

which, due to (4.4), is reachable only when $h_i > 1$. In such a case, for any greater value of a_i there are no possible values of σ_i. Again, by (4.4) we conclude that, after reaching the point of complete failure of a spring, the solution is either not continuable, or there is no more evolution in the respective component of the solution:

$$\begin{aligned} &\text{Equation (4.5) is true for some } i \in \overline{1,m},\ t^* \in [0,T], \\ &\qquad h_i > 1, \qquad\qquad \Longrightarrow \quad \text{for a.a. } t \geqslant t^* \text{ we have } \dot{a}_i = \dot{\sigma}_i = 0. \\ &\text{but the solution exists on } [0,T] \end{aligned} \tag{4.6}$$

4.1.2. Geometric compatibility, displacement load and the well-posedness assumptions

To reflect the fact that the springs are required to stay connected according to the given graph at all times, we proceed to construct the linearized compatibility equation.

To each of the m springs of the lattice we assign an arbitrary orientation, by calling one of its endpoints the *origin* and the other one the *terminus* [19, Chapter 7], constructing a *directed graph* in this manner. The structure of the lattice can then be described by an $n \times m$ incidence matrix Q of the directed graph. The incidence matrix is constructed as the following (see more details in [5]): For $i \in \overline{1,m}$, $j \in \overline{1,n}$ set

- $Q_{ji} = 0$ if none of the endpoints of spring i is node j,
- $Q_{ji} = 1$ if node j is the origin of the spring i according to the assigned orientation,
- $Q_{ji} = -1$ if node j is the terminus of the spring i according to the assigned orientation.

At any particular moment the coordinates of the vertices can be collected into a vector $\xi \in \mathbb{R}^{nd}$ so that $\xi_{d(j-1)+k}$ is the k-th coordinate of the node j (where $j \in \overline{1,n}, k \in \overline{1,d}$). The length of spring i (where $i \in \overline{1,m}$) can then be calculated as the norm of the vector

$$\text{(the terminus of spring } i\text{)} - \text{(the origin of spring } i\text{)} = -\left(\sum_{j=1}^{n} Q_{ji}\xi_{d(j-1)+k}\right)_{k\in\overline{1,d}}$$

and the lengths of all m springs can be calculated by the function

$$\varphi : \mathbb{R}^{nd} \to \mathbb{R}^{m}$$

$$\varphi(\xi) = (\varphi_i(\xi))_{i\in\overline{1,m}} := \left(\sqrt{\sum_{k=1}^{d}\left(\sum_{j=1}^{n} Q_{ji}\xi_{d(j-1)+k}\right)^2}\right)_{i\in\overline{1,m}}. \tag{4.7}$$

We linearize function φ at a given fixed *reference configuration* $\xi_0 = (\xi^0_{d(j-1)+k}) \in \mathbb{R}^{nd}$ and write down the *geometric constraint* connecting x and the vector of *displacements* $\zeta \in \mathbb{R}^{nd}$ of the nodes from the reference configuration:

$$\left(D_{\xi_0}\varphi\right)\zeta = x. \tag{LSM4}$$

Here both x and ζ are unknown variables but we assume that displacements ζ are small compared to the lengths of the springs, therefore, we can use fixed ξ_0. Jacobi matrix $D_{\xi_0}\varphi$ in (LSM4) is independent on t, and it can be written explicitly. Specifically, the $(i, d(j-1)+k)$ entry of $D_{\xi_0}\varphi$ is given by

$$\left.\frac{\partial\varphi_i}{\partial\xi_{d(j-1)+k}}\right|_{\xi=\xi_0} = \frac{\left(\sum\limits_{\bar{j}=1}^{n} Q_{\bar{j}i}\xi^0_{d(\bar{j}-1)+k}\right)Q_{ji}}{\sqrt{\sum\limits_{\bar{k}=1}^{d}\left(\sum\limits_{\bar{j}=1}^{n} Q_{\bar{j}i}\xi^0_{d(\bar{j}-1)+\bar{k}}\right)^2}} = \mathcal{D}_{ik}Q_{ji}, \tag{4.8}$$

where $\mathcal{D}$ is the $m \times d$-matrix with (i,k) entry

$$\mathcal{D}_{ik} = \frac{1}{\varphi_i(\xi_0)}\sum_{\bar{j}=1}^{n} Q_{\bar{j}i}\xi^0_{d(\bar{j}-1)+k}. \tag{4.9}$$

Observe that i-th row of $\mathcal{D}$ is the *unit vector in the direction from the terminus to the origin of spring i in reference configuration* ξ_0, i.e., the direction of such unit vector is opposite to the chosen orientation in the geometric directed graph, corresponding to Q with the nodes placement ξ_0.

Equation (LSM4) appears in the literature [55, (2.6)] and [63, (3.17)] (in the form for individual springs).

Along with the geometric constraint we introduce an additional constraint to play the role of the boundary condition. It has the form

$$R(\xi_0 + \zeta) + r(t) = 0, \tag{LSM5}$$

where R is a given $q \times nd$-matrix and r is a given function of time with q-vector values for some $q \in \mathbb{N}$. We call equation (LSM5), function r and number q, respectively, the *external displacement constraint*, the *displacement load* and the *number of external displacement constraints*. In turn, vectors $\zeta \in \mathbb{R}^{nd}$ satisfying (LSM5) we call *feasible displacements*.

For well-posedness of the problem we need the following assumptions about given data R and $D_{\xi_0}\varphi$ to hold:

Assumption 1. *Well-definiteness of the external constraint, i.e., the matrix R has maximum row rank:*

$$\operatorname{rank} R = q. \tag{4.10}$$

Assumption 2. *Kinematic determinacy, which means that it is possible to uniquely solve* (LSM4)–(LSM5) *for displacements ζ (hence, for the positions $\xi_0 + \zeta$ of the nodes) when elongation values x are already obtained. In the next Section 4.1.3 this condition also allows us to apply external forces of any direction. Kinematic determinacy can be written mathematically as the following equivalent conditions:*

$$\operatorname{rank} \begin{pmatrix} (D_{\xi_0}\varphi)^\top & R^\top \end{pmatrix} = nd, \tag{4.11}$$

$$\operatorname{Ker} \begin{pmatrix} D_{\xi_0}\varphi \\ R \end{pmatrix} = \{0\},$$

$$\operatorname{Ker}(D_{\xi_0}\varphi) \cap \operatorname{Ker} R = \{0\}. \tag{4.12}$$

Matrices $D_{\xi_0}\varphi$ and $\begin{pmatrix} D_{\xi_0}\varphi \\ R \end{pmatrix}$ we call, respectively, *the compatibility matrix* and *the enhanced compatibility matrix* of the lattice defined by Q, ξ_0, R and r. In turn, the matrices $(D_{\xi_0}\varphi)^\top$, $\begin{pmatrix} (D_{\xi_0}\varphi)^\top & R^\top \end{pmatrix}$ we call, respectively *the equilibrium matrix* and *the enhanced equilibrium matrix* of the lattice. The image of the map φ (4.7) is a nonlinear surface, known as the *Cayley-Menger variety* [33, p. 435], and the linearization (LSM4) to its tangent space (see [1, Figure 1, p. 78]) plays the central role in rigidity theory [2, Chapter 9]. We refer to [38, Section 3] for more references and a comprehensive overview of the algebraic properties (LSM4) and (LSM5) in relation to the kinematic properties of the lattice. Assumption 2 is also discussed there in the context of rigidity theory.

4.1.3. Equation of equilibrium

We model the *quasi-static* evolution, meaning that the lattice stays at an equilibrium at all times. Specifically, we refer to the following:

Definition 4.1. [35, p. 17] A system of m particles is said to be at an *equilibrium* when the total force on each particle vanishes.

In our case the nodes of the lattice serve as particles, and the equation of equilibrium in the following form can be derived from (LSM4) and (LSM5) using the principle of virtual work (see [38, Section 3] for the complete derivation):

$$(D_{\xi_0}\varphi)^\top(-\sigma + F_1 f(t)) \in \operatorname{Im} R^\top, \tag{LSM6}$$

where $f(t) \in \mathbb{R}^{nd}$ is a given function of time, which we call the *stress load* or the *external force*. For a fixed t vector $f(t)$ has the following physical meaning: $f_{d(j-1)+k}$ is the k-th component of the force vector, applied to node j ($j \in \overline{1,n}, k \in \overline{1,d}$). In turn, F_1 is an $(nd) \times m$-matrix, obtained as the following. The enhanced equilibrium matrix $\begin{pmatrix}(D_{\xi_0}\varphi)^\top & R^\top\end{pmatrix}$ has dimensions $(nd) \times (m+q)$, and, by assumption (4.11) it has full row rank. Therefore, its Moore-Penrose pseudoinverse matrix $\begin{pmatrix}(D_{\xi_0}\varphi)^\top & R^\top\end{pmatrix}^+$ is also a right inverse and can be explicitly written [38, Proposition 2.3] as

$$\begin{pmatrix}(D_{\xi_0}\varphi)^\top & R^\top\end{pmatrix}^+ = \begin{pmatrix}F_1\\F_2\end{pmatrix} = \begin{pmatrix}D_{\xi_0}\varphi\\R\end{pmatrix}\left(\begin{pmatrix}(D_{\xi_0}\varphi)^\top & R^\top\end{pmatrix}\begin{pmatrix}D_{\xi_0}\varphi\\R\end{pmatrix}\right)^{-1}, \tag{4.13}$$

where F_1 and F_2 are $m \times (nd)$ and $q \times (nd)$ matrices, respectively.

Equation (LSM6) is a slightly modified version of equations from the literature [55, (2.4)] and [63, (3.23)].

4.1.4. The complete set of equations of the elasto-plastic Lattice Spring Model with variable set of admissible stresses

Naturally, we require the regularity of the displacement and stress load function:

Assumption 3. *We assume that $r : [0,T] \to \mathbb{R}^q$ and $f : [0,T] \to \mathbb{R}^{nd}$ are absolutely continuous.*

We summarize the mathematical formulation of the problem of the quasistatic evolution of an elasto-plastic Lattice Spring Model. Given finctions r, f (displacement and stress loads, respectively) find unknown functions $x, \varepsilon, p, \sigma, a : [0,T] \to \mathbb{R}^m, \zeta : [0,T] \to \mathbb{R}^{nd}$ such that for all $t \in [0,T]$

$$\text{Additive decomposition:} \qquad x = \varepsilon + p, \tag{LSM1}$$

$$\text{Hooke's law:} \qquad \sigma = K\varepsilon, \tag{LSM2}$$

$$\text{Geometric constraint:} \qquad \left(D_{\xi_0}\varphi\right)\zeta = x \tag{LSM4}$$

$$\text{External displacement constraint:} \qquad R(\xi_0 + \zeta) + r(t) = 0, \tag{LSM5}$$

$$\text{Equation of equilibrium:} \qquad (D_{\xi_0}\varphi)^\top(-\sigma + F_1 f(t)) \in \operatorname{Im} R^\top, \tag{LSM6}$$

and for a.a. $t \in [0,T]$

$$\text{State-dependent plastic flow rule:} \qquad \frac{d}{dt}\begin{pmatrix}p\\-a\end{pmatrix} \in N_{\mathrm{C}+\begin{pmatrix}0\\Ha\end{pmatrix}}\begin{pmatrix}\sigma\\a\end{pmatrix}. \tag{LSM3}$$

4.2. Derivation of the state-dependent sweeping process from the equations of the lattice

Before we proceed to the sweeping process, we will need some technical definitions and facts. Define the subspaces of $\mathbb{R}^m$

$$\mathcal{U} = K(D_{\xi_0}\varphi)\operatorname{Ker} R, \tag{4.14}$$

$$\mathcal{V} = \{\sigma \in \mathbb{R}^m : (D_{\xi_0}\varphi)^\top \sigma \in \operatorname{Im} R^\top\} \tag{4.15}$$

and introduce the inner product $\langle \cdot, \cdot \rangle_{K^{-1}}$ in $\mathbb{R}^m$ as

$$\langle x, y \rangle_{K^{-1}} = x^\top K^{-1} y. \tag{4.16}$$

The following proposition establishes the essential properties of $\mathcal{U}$ and $\mathcal{V}$.

Proposition 4.1. *Provided that assumptions* (4.10) *and* (4.11) *hold true, the following is true as well.*

i) The orthogonal complement of $\mathcal{V} \subset \mathbb{R}^m$ in the sense of the standard inner product in $\mathbb{R}^m$ is

$$\mathcal{V}^\perp = (D_{\xi_0}\varphi) \operatorname{Ker} R, \tag{4.17}$$

and the orthogonal complement of $\mathcal{V} \subset \mathbb{R}^m$ in the sense of the inner product (4.16) *is $\mathcal{U}$.*

ii) The set of σ's satisfying equilibrium Eq (LSM6) *is an affine translation of space $\mathcal{V}$. Specifically, for any $\sigma \in \mathbb{R}^m$ and any t*

$$\sigma \textit{ satisfies } (\text{LSM6}) \quad \Longleftrightarrow \quad \sigma \in \mathcal{V} + F_1 f(t).$$

iii) The dimensions of $\mathcal{U}$ and $\mathcal{V}$ are

$$\dim \mathcal{U} = nd - q, \qquad \dim \mathcal{V} = m - nd + q.$$

Proof. *i)* Observe that

$$\begin{aligned}
((D_{\xi_0}\varphi) \operatorname{Ker} R)^\perp &= \{x \in \mathbb{R}^m : x^\top (D_{\xi_0}\varphi) y = 0 \text{ for all } y \in \operatorname{Ker} R\} \\
&= \{x \in \mathbb{R}^m : \left((D_{\xi_0}\varphi)^\top x\right)^\top y = 0 \text{ for all } y \in \operatorname{Ker} R\} \\
&= \{x \in \mathbb{R}^m : (D_{\xi_0}\varphi)^\top x \in (\operatorname{Ker} R)^\perp\} \\
&= \{x \in \mathbb{R}^m : (D_{\xi_0}\varphi)^\top x \in \operatorname{Im} R^\top\} \\
&= \mathcal{V},
\end{aligned}$$

which proves the first statement about the standard inner product. Since

$$x \in \mathcal{V}^\perp \quad \Longleftrightarrow \quad x^\top \sigma = 0 \text{ for all } \sigma \in \mathcal{V}$$

therefore

$$Kx \in K\mathcal{V}^\perp \quad \Longleftrightarrow \quad (Kx)^\top K^{-1} \sigma = 0 \text{ for all } \sigma \in \mathcal{V},$$

which proves the statement about the inner product (4.16).

ii) This can be verified by substituting $\sigma - F_1 f(t)$ as σ into definition (4.15) of $\mathcal{V}$.

iii) By rank-nullity theorem [67, Theorem 2.49], assumption (4.10) implies that $\dim \operatorname{Ker} R = nd - q$, therefore, if we take a basis of $\operatorname{Ker} R$ and arrange its vectors as columns in a matrix R_0, we get $m \times (nd - q)$ matrix R_0 with linearly independent columns. Observe that it follows from definition (4.14) of $\mathcal{U}$ and from (4.12) that $\dim \mathcal{U} = \dim \operatorname{Ker} R = nd - q$. Indeed, assume that $\dim \mathcal{U} < \dim \operatorname{Ker} R$. Then there is a nontrivial linear combination of basis vectors of $\operatorname{Ker} R$ (i.e., $R_0 z$ with a vector of coefficients $z \in \mathbb{R}^{nd-q} \setminus \{0\}$) such that $K(D_{\xi_0}\varphi)R_0 z = 0$, i.e., the vector $R_0 z$ belongs to $\operatorname{Ker}(D_{\xi_0}\varphi)$. Since $R_0 z$ is also from $\operatorname{Ker} R$ by construction, we have a contradiction with (4.12).

□

We call space $\mathcal{V}$ *the space of self-stresses* of the lattice, as it represents all such stress vectors $\sigma \in \mathbb{R}^m$ for which the corresponding forces, exerted by the springs to the nodes, either vanish or can be compensated by the reactions of the external displacement constraint (LSM5). For a more comprehensive discussion of the self-stresses and their connection to rigidity of the lattice we refer to [38, Section 3] and the references therein.

Space $\mathcal{V}$ is a central element of our further construction, and in order to have a meaningful problem we assume that $\mathcal{V}$ has a dimension of at least one (in addition to the assumptions (4.10) and (4.11)):

Assumption 4. *Non-degeneracy of the space of self-stresses:*

$$nd - q < m. \tag{4.18}$$

Put differently, (4.18) means that for each stress load $f(t)$ there is more than just one stress vector $\sigma \in \mathbb{R}^m$ which brings the lattice to the equilibrium, i.e., we assume that the lattice is not *statically determinate*.

For further use we need to define several matrices.

$R^+ = R^\top (RR^\top)^{-1}$	is the $nd \times q$ Moore-Penrose pseudoinverse matrix of R (see [38, Section 2.2]),
U	is an $m \times \dim \mathcal{U}$ matrix composed of columns which form a basis in $\mathcal{U}$,
V	is an $m \times \dim \mathcal{V}$ matrix composed of columns which form a basis in $\mathcal{V}$.

Then there are matrices P_U and P_V such that UP_U and VP_V form a pair of projection maps, orthogonal in the sense of (4.16). Namely (see [67, Sections 5.3 and 5.4]),

$$P_U = \left(U^\top K^{-1} U\right)^{-1} U^\top K^{-1} \qquad P_V = \left(V^\top K^{-1} V\right)^{-1} V^\top K^{-1}. \tag{4.19}$$

Finally, let

$$G = VP_V K(D_{\xi_0}\varphi)R^+, \tag{4.20}$$

$$F = UP_U F_1, \tag{4.21}$$

and now we can convert the problem (LSM1)–(LSM6) to a state-dependent sweeping process.

Theorem 4.1. *Let Assumptions 1–4 hold true and let $s_i > 0$ for all $i \in \overline{1,m}$. The following statements are equivalent:*

i) Absolutely continuous functions $x, \varepsilon, p, \sigma, a : [0,T] \to \mathbb{R}^m$, $\zeta : [0,T] \to \mathbb{R}^{nd}$ solve (LSM1)–(LSM6) *and y is defined as*

$$y = \sigma + Gr(t) - Ff(t). \tag{4.22}$$

ii) Absolutely continuous function $\begin{pmatrix} y \\ a \end{pmatrix} : [0,T] \to \mathbb{R}^{2m}$ is a solution of state-dependent sweeping process

$$-\frac{d}{dt}\begin{pmatrix} y \\ a \end{pmatrix} \in N^{\mathbb{K}^{-1}}_{C(t,a)}\begin{pmatrix} y \\ a \end{pmatrix}, \tag{4.23}$$

where

$$\mathbb{K} = \begin{pmatrix} K & 0 \\ 0 & I \end{pmatrix}, \qquad C(t,a) = \left(\mathrm{C} + \begin{pmatrix} Gr(t) - Ff(t) \\ Ha \end{pmatrix} \right) \cap (\mathcal{V} \times \mathbb{R}^m), \tag{4.24}$$

where C *is given by* (4.1)*, and*

$$\sigma = y - Gr(t) + Ff(t), \tag{4.25}$$

$$\varepsilon = K^{-1}\sigma, \tag{4.26}$$

$$p(t) = p(0) + \int_0^t \operatorname{diag}\left(\frac{\operatorname{sign} \sigma_i(\tau)}{s_i} \right) \dot{a}(\tau) d\tau, \tag{4.27}$$

$$x = \varepsilon + p, \tag{LSM1}$$

$$\zeta = \begin{pmatrix} D_{\xi_0}\varphi \\ R \end{pmatrix}^{+} \begin{pmatrix} x \\ -R\xi_0 - r(t) \end{pmatrix}, \tag{4.28}$$

$$\begin{pmatrix} D_{\xi_0}\varphi \\ R \end{pmatrix} \zeta(0) = \begin{pmatrix} x(0) \\ -R\xi_0 - r(0) \end{pmatrix}, \tag{4.29}$$

where $\begin{pmatrix} D_{\xi_0}\varphi \\ R \end{pmatrix}^{+}$ *is the Moore-Penrose pseudoinverse matrix of* $\begin{pmatrix} D_{\xi_0}\varphi \\ R \end{pmatrix}$*, which in our case (due to* (4.11)*) can be explicitly written as*

$$\begin{pmatrix} D_{\xi_0}\varphi \\ R \end{pmatrix}^{+} = \left(\begin{pmatrix} (D_{\xi_0}\varphi)^\top & R^\top \end{pmatrix} \begin{pmatrix} D_{\xi_0}\varphi \\ R \end{pmatrix} \right)^{-1} \begin{pmatrix} (D_{\xi_0}\varphi)^\top & R^\top \end{pmatrix}. \tag{4.30}$$

If $s_i = 0$ *for some* $i \in \overline{1,m}$ *we only claim that* (LSM1)–(LSM6)*,* (4.22) $\Longrightarrow$ (4.23) *and* (4.24)*.*

Remark 4.3. Formula (4.23) implies that the initial state is admissible, i.e.,

$$\begin{pmatrix} y(0) \\ a(0) \end{pmatrix} \in C(0, a(0)). \tag{4.31}$$

Remark 4.4. Moving set $C(t,a)$ in (4.24) can be written in the several following ways. At first, observe that

$$C(t,\tilde{a}) = \left\{ \begin{pmatrix} y \\ a \end{pmatrix} \in \mathcal{V} \times \mathbb{R}^m : \begin{array}{c} -(y_i - (Gr(t) - Ff(t))_i) - s_i(a_i - h_i\tilde{a}_i) \leqslant c_{0,i}, \\ (y_i - (Gr(t) - Ff(t))_i) - s_i(a_i - h_i\tilde{a}_i) \leqslant c_{0,i} \end{array} \text{ for all } i \in \overline{1,m} \right\}, \tag{4.32}$$

which is the same as

$$C(t,\tilde{a}) = \left\{ \begin{pmatrix} y \\ a \end{pmatrix} \in \mathcal{V} \times \mathbb{R}^m : \begin{array}{c} \begin{pmatrix} -k_i e_i \\ -s_i e_i \end{pmatrix}^\top \mathbb{K}^{-1} \begin{pmatrix} y - (Gr(t) - Ff(t)) \\ a - H\tilde{a} \end{pmatrix} \leqslant c_{0,i}, \\ \begin{pmatrix} k_i e_i \\ -s_i e_i \end{pmatrix}^\top \mathbb{K}^{-1} \begin{pmatrix} y - (Gr(t) - Ff(t)) \\ a - H\tilde{a} \end{pmatrix} \leqslant c_{0,i} \end{array} \text{ for all } i \in \overline{1,m} \right\}, \tag{4.33}$$

where by e_i we denote the i-th vector of the standard basis in $\mathbb{R}^m$.

Furthermore, we would like to have the definition of $C(t,\tilde{a})$ with the normal vectors from within linear space $\mathcal{V}\times\mathbb{R}^m$. For that we can utilize the the variational definition of orthogonal projection [12, Corollary 5.4, p. 134] and replace k_ie_i with $k_iVP_Ve_i$, however due to $Ff(t)\notin\mathcal{V}$ we can only write

$$C(t,\tilde{a})=\left\{\begin{pmatrix}y\\a\end{pmatrix}\in\mathcal{V}\times\mathbb{R}^m:\ \begin{matrix}n_{-i}^\top\mathbb{K}^{-1}\begin{pmatrix}y-Gr(t)\\a-H\tilde{a}\end{pmatrix}-(Ff(t))_i\leqslant c_{0,i},\\ n_{+i}^\top\mathbb{K}^{-1}\begin{pmatrix}y-Gr(t)\\a-H\tilde{a}\end{pmatrix}+(Ff(t))_i\leqslant c_{0,i}\end{matrix}\quad\text{for all } i\in\overline{1,m}\right\},\tag{4.34}$$

where

$$n_{-i}=\begin{pmatrix}-k_iVP_V\,e_i\\-s_ie_i\end{pmatrix}\in\mathcal{V}\times\mathbb{R}^m,\qquad n_{+i}=\begin{pmatrix}k_iVP_V\,e_i\\-s_ie_i\end{pmatrix}\in\mathcal{V}\times\mathbb{R}^m.\tag{4.35}$$

Thus, we can write another expression of the set as

$$C(t,\tilde{a})=C^f(t)+\begin{pmatrix}Gr(t)\\H\tilde{a}\end{pmatrix},\tag{4.36}$$

where

$$C^f(t)=\left\{\begin{pmatrix}y\\a\end{pmatrix}\in\mathcal{V}\times\mathbb{R}^m:\ \begin{matrix}n_{-i}^\top\mathbb{K}^{-1}\begin{pmatrix}y\\a\end{pmatrix}\leqslant c_{0,i}+(Ff(t))_i,\\ n_{+i}^\top\mathbb{K}^{-1}\begin{pmatrix}y\\a\end{pmatrix}\leqslant c_{0,i}-(Ff(t))_i\end{matrix}\quad\text{for all } i\in\overline{1,m}\right\},\tag{4.37}$$

which highlights that the damage state $\tilde{a}$ and the displacement loading $Gr(t)$ affect $C(t,\tilde{a})$ as parallel translations.

Finally, for our convenience, we introduce the notation

$$C(t,\tilde{a})=\left\{\begin{pmatrix}y\\a\end{pmatrix}\in\mathcal{V}\times\mathbb{R}^m:\ \begin{matrix}g_{-i}\left(t,\tilde{a},\begin{pmatrix}y\\a\end{pmatrix}\right)\leqslant 0,\\ g_{+i}\left(t,\tilde{a},\begin{pmatrix}y\\a\end{pmatrix}\right)\leqslant 0\end{matrix}\quad\text{for all } i\in\overline{1,m}\right\},$$

$$\begin{aligned}g_{-i}\left(t,\tilde{a},\begin{pmatrix}y\\a\end{pmatrix}\right)&=-(y_i-(Gr(t)-Ff(t))_i)-s_i(a_i-h_i\tilde{a}_i)-c_{0,i}\\&=n_{-i}^\top\mathbb{K}^{-1}\begin{pmatrix}y-Gr(t)\\a-H\tilde{a}\end{pmatrix}-(Ff(t))_i-c_{0,i},\end{aligned}\tag{4.38}$$

$$\begin{aligned}g_{+i}\left(t,\tilde{a},\begin{pmatrix}y\\a\end{pmatrix}\right)&=(y_i-(Gr(t)-Ff(t))_i)-s_i(a_i-h_i\tilde{a}_i)-c_{0,i}\\&=n_{+i}^\top\mathbb{K}^{-1}\begin{pmatrix}y-Gr(t)\\a-H\tilde{a}\end{pmatrix}+(Ff(t))_i-c_{0,i}.\end{aligned}\tag{4.39}$$

The statement and the proof of Theorem 4.1 are similar to [38, Theorem 5.1] and [39, Theorem 3.1]. There we considered lattices with elastic-perfectly plastic springs and proved the implication similar to *i)⇒ii)*. However, current Theorem 4.1 covers all the cases of hardening, perfect plasticity and softening in a uniform manner, and we are able to prove the two-sided statement *i)⇔ii)*.

Proof of Theorem 4.1. **From the LSM** *i)* **to the Sweeping Process** *ii)***.** To show (4.23) and (4.24) we only need $s_i \geqslant 0$ for all $i \in \overline{1,m}$. We start by transforming the relations (LSM4)–(LSM6) into inclusions in terms of spaces $\mathcal{U}$ and $\mathcal{V}$, respectively.

We fix a.e. $t \in [0,T]$, take time-detivative of (LSM5) and apply the Moore-Penrose pseudoinverse matrix R^+ of R to it:

$$R^+R\dot{\zeta} + R^+\dot{r}(t) = 0.$$

Matrix R^+R is the orthogonal projection matrix onto $\operatorname{Im} R^\top$ ([15, Definition 1.1.2]), therefore, there is $z \in (\operatorname{Im} R^\top)^\perp = \operatorname{Ker} R$, s.t. $\dot{\zeta} = R^+R\dot{\zeta} + z$ and

$$\dot{\zeta} - z + R^+\dot{r}(t) = 0.$$

Apply $K(D_{\xi_0}\varphi)$:

$$K(D_{\xi_0}\varphi)\dot{\zeta} - K(D_{\xi_0}\varphi)z + K(D_{\xi_0}\varphi)R^+\dot{r}(t) = 0,$$

and from (LSM4) and (4.14) we get

$$K\dot{x} \in \mathcal{U} - K(D_{\xi_0}\varphi)R^+\dot{r}(t). \tag{4.40}$$

The last term can be represented as the sum of projections:

$$K\dot{x} \in \mathcal{U} - (UP_U + VP_V)K(D_{\xi_0}\varphi)R^+\dot{r}(t).$$

Hence

$$K\dot{x} \in \mathcal{U} - VP_VK(D_{\xi_0}\varphi)R^+\dot{r}(t),$$

i.e.,

$$K\dot{x} \in \mathcal{U} - G\dot{r}(t). \tag{4.41}$$

On the other hand, as we observed in Proposition 4.1 *ii)*, Eq (LSM6) means precisely that

$$-\sigma + F_1f(t) \in \mathcal{V} \tag{4.42}$$

i.e.,

$$-y + Gr(t) - (UP_U + VP_V)Ff(t) + F_1f(t) \in \mathcal{V} \tag{4.43}$$

and by collecting all the terms from $\mathcal{V}$ and using (4.21) we get that

$$-y \in \mathcal{V},$$

$$y \in \mathcal{V}. \tag{4.44}$$

At last, from (LSM1) and (LSM2) we see that

$$Kp = Kx - \sigma.$$

Then, using (2.3), we can write (LSM3) as

$$\frac{d}{dt}\begin{pmatrix} Kx - \sigma \\ -a \end{pmatrix} \in N^{\mathbb{K}^{-1}}_{\mathrm{C}+\begin{pmatrix} 0 \\ Ha \end{pmatrix}}\begin{pmatrix} \sigma \\ a \end{pmatrix},$$

$$\frac{d}{dt}\begin{pmatrix}-\sigma\\-a\end{pmatrix} \in N^{\mathbb{K}^{-1}}_{\mathrm{C}+\begin{pmatrix}0\\Ha\end{pmatrix}}\begin{pmatrix}\sigma\\a\end{pmatrix} - \begin{pmatrix}K\dot{x}\\0\end{pmatrix}.$$

Plug (4.41) and (4.25),

$$\frac{d}{dt}\begin{pmatrix}-y\\-a\end{pmatrix} + \begin{pmatrix}G\dot{r}(t)\\0\end{pmatrix} - \begin{pmatrix}F\dot{f}(t)\\0\end{pmatrix} \in N^{\mathbb{K}^{-1}}_{\mathrm{C}+\begin{pmatrix}0\\Ha\end{pmatrix}}\begin{pmatrix}y - Gr(t) + Ff(t)\\a\end{pmatrix} - \mathcal{U}\times\{0_m\} + \begin{pmatrix}G\dot{r}(t)\\0\end{pmatrix}.$$

Cancel the term with $G\dot{r}(t)$ and use the fact that $F\dot{f}(t) \in \mathcal{U}$:

$$-\frac{d}{dt}\begin{pmatrix}y\\a\end{pmatrix} \in N^{\mathbb{K}^{-1}}_{\mathrm{C}+\begin{pmatrix}0\\Ha\end{pmatrix}}\begin{pmatrix}y - Gr(t) + Ff(t)\\a\end{pmatrix} - \mathcal{U}\times\{0_m\}. \tag{4.45}$$

Due to (4.44) and Proposition 4.1 *i)* we have

$$-\mathcal{U}\times\{0_m\} = \mathcal{U}\times\{0_m\} = N^{\mathbb{K}^{-1}}_{\mathcal{V}\times\mathbb{R}^m}\begin{pmatrix}y\\a\end{pmatrix},$$

therefore, also by using (2.2), we get

$$-\frac{d}{dt}\begin{pmatrix}y\\a\end{pmatrix} \in N^{\mathbb{K}^{-1}}_{\mathrm{C}+\begin{pmatrix}Gr(t) - Ff(t)\\Ha\end{pmatrix}}\begin{pmatrix}y\\a\end{pmatrix} + N^{\mathbb{K}^{-1}}_{\mathcal{V}\times\mathbb{R}^m}\begin{pmatrix}y\\a\end{pmatrix}. \tag{4.46}$$

Due to the additivity of the normal cones to polyhedral sets [71, Corollary 23.8.1], we obtain

$$-\frac{d}{dt}\begin{pmatrix}y\\a\end{pmatrix} \in N^{\mathbb{K}^{-1}}_{\left(\mathrm{C}+\begin{pmatrix}Gr(t) - Ff(t)\\Ha\end{pmatrix}\right)\cap(\mathcal{V}\times\mathbb{R}^m)}\begin{pmatrix}y\\a\end{pmatrix},$$

which is exactly (4.23)-(4.24).

Equations (4.25), (4.26) and (LSM1) follow trivially from *i)*.

Now we assume that $s_i > 0$ for all $i \in \overline{1,m}$ and we proceed to show (4.27)–(4.29). Notice from (LSM3) and (4.3) that for all $i \in \overline{1,m}$ a.a. $t \in [0,T]$,

$$\frac{d}{dt}\begin{pmatrix}p_i\\-a_i\end{pmatrix} = \lambda_i^-\begin{pmatrix}-1\\-s_i\end{pmatrix} + \lambda_i^+\begin{pmatrix}1\\-s_i\end{pmatrix} \qquad \text{for some } t\text{-dependent } \lambda_i^-, \lambda_i^+ \geqslant 0.$$

Observe that $\lambda_i^- > 0$ and $\lambda_i^+ > 0$ simultaneously is possible only when both equalities of (4.5) hold true, and only when $h_i > 1$ (see Figure 5f). Thus, it is the state of complete failure, i.e., we can use the implication (4.6) to deduce that

$$\lambda_i^- = \lambda_i^+ = 0 = \dot{p}_i.$$

Otherwise

$$\lambda_i = \frac{\dot{a}_i}{s_i}, \qquad \dot{p}_i = \mp\lambda_i \qquad \text{for some } \lambda_i \geqslant 0.$$

More specifically,

$$\dot{p}_i = \begin{cases} -\frac{\dot{a}_i}{s_i} & \text{if} \quad -\sigma_i - s_i(1-h_i)a_i = c_{0,i}, \\ \frac{\dot{a}_i}{s_i} & \text{if} \quad \sigma_i - s_i(1-h_i)a_i = c_{0,i}, \\ 0 & \text{otherwise.} \end{cases} = \begin{cases} -\frac{\dot{a}_i}{s_i} & \text{if} \quad g_{-i}\left(t, a, \begin{pmatrix} y \\ a \end{pmatrix}\right) = 0, \\ \frac{\dot{a}_i}{s_i} & \text{if} \quad g_{+i}\left(t, a, \begin{pmatrix} y \\ a \end{pmatrix}\right) = 0, \\ 0 & \text{otherwise.} \end{cases} \tag{4.47}$$

Equivalently, we can write

$$\dot{p}_i = \frac{\dot{a}_i}{s_i}\operatorname{sign}(\sigma_i) = \frac{\dot{a}_i}{s_i}\operatorname{sign}\left(y_i - (Gr(t) - Ff(t))_i\right), \tag{4.48}$$

where the sign function is used to determine which of the equalities in (4.5) holds (if neither then $\dot{a}_i = \dot{p}_i = 0$ anyways). Expression (4.27) follows.

Finally, from (LSM4) and (LSM5) we have

$$\begin{pmatrix} D_{\xi_0}\varphi \\ R \end{pmatrix}\zeta = \begin{pmatrix} x \\ -R\xi_0 - r(t) \end{pmatrix}, \tag{4.49}$$

where $(m+q)\times(nd)$ enhanced compatibility matrix $\begin{pmatrix} D_{\xi_0}\varphi \\ R \end{pmatrix}$ has full column rank due to assumption (4.11). Thus, its Moore-Penrose pseudoinverse matrix is a left inverse and can be computed as (4.30), see [38, Prop. 2.3]. Expression (4.28) for ζ then follows immediately, and (4.29) is trivially implied by (4.49) as well.

From the Sweeping Process *ii)* to the LSM *i)*. Let $s_i > 0$ for all $i \in \overline{1,m}$ and assume that initial data satisfy (4.29). Let $\begin{pmatrix} y \\ a \end{pmatrix}$ be a solution of (4.23) and (4.24) on $[0,T]$ and compute $\sigma, \varepsilon, p, x, \zeta$ by (4.25)–(4.28) and (LSM1). We immediately have (LSM1) and (LSM2). From (4.23) and (4.24), we necessarily have (4.44), which can be transformed back to (4.43), then to (4.42), which is, again, equivalent to (LSM6).

Furthermore, (4.48) follows from (4.27). Similarly to Remark 4.1, we see that sweeping process (4.23) implies $\dot{a}_i \geqslant 0$. As above, we do not consider the state of complete failure, and from (4.48) we deduce (4.47), which, in turn, means that (LSM3) is satisfied with (4.2) and (4.3).

We need to show that (LSM4) and (LSM5) hold. From (4.23) we can go back to (4.46), and then to (4.45), in which we plug (4.22) to get

$$-\frac{d}{dt}\begin{pmatrix} \sigma + Gr(t) - Ff(t) \\ a \end{pmatrix} \in N^{\mathbb{K}^{-1}}_{\mathrm{C}+\begin{pmatrix} 0 \\ Ha \end{pmatrix}}\begin{pmatrix} \sigma \\ a \end{pmatrix} - \mathcal{U}\times\{0_m\}.$$

Since we have (LSM1) and (LSM2), we can write

$$\sigma = Kx - Kp.$$

Hence, knowing that $F\dot{f}(t) \in \mathcal{U}$,

$$-\frac{d}{dt}\begin{pmatrix} Kx + Gr(t) \\ 0 \end{pmatrix} + \frac{d}{dt}\begin{pmatrix} Kp \\ -a \end{pmatrix} \in N^{\mathbb{K}^{-1}}_{\mathrm{C}+\begin{pmatrix} 0 \\ Ha \end{pmatrix}}\begin{pmatrix} \sigma \\ a \end{pmatrix} - \mathcal{U}\times\{0_m\}.$$

We already have proven (LSM3), which together with (2.3) allows us to write

$$-\frac{d}{dt}\begin{pmatrix} Kx + Gr(t) \\ 0 \end{pmatrix} \in N^{\mathbb{K}^{-1}}_{\mathrm{C}+\begin{pmatrix} 0 \\ Ha \end{pmatrix}} \begin{pmatrix} \sigma \\ a \end{pmatrix} - \mathcal{U} \times \{0_m\},$$

i.e., there are two components $\begin{pmatrix} w_1 \\ \beta_1 \end{pmatrix}, \begin{pmatrix} w_2 \\ 0 \end{pmatrix} \in \mathbb{R}^{2m}$ such that

$$\begin{pmatrix} w_1 \\ \beta_1 \end{pmatrix} + \begin{pmatrix} w_2 \\ 0 \end{pmatrix} = -\frac{d}{dt}\begin{pmatrix} Kx + Gr(t) \\ 0 \end{pmatrix}, \qquad \begin{pmatrix} w_1 \\ \beta_1 \end{pmatrix} \in N^{\mathbb{K}^{-1}}_{\mathrm{C}+\begin{pmatrix} 0 \\ Ha \end{pmatrix}} \begin{pmatrix} \sigma \\ a \end{pmatrix}, \qquad \begin{pmatrix} w_2 \\ 0 \end{pmatrix} \in \mathcal{U} \times \{0_m\}. \tag{4.50}$$

Hence $\beta_1 = 0$. But, notice from (4.3), that the only element of the normal cone $N_{\mathrm{C}+\begin{pmatrix} 0 \\ Ha \end{pmatrix}} \begin{pmatrix} \sigma \\ a \end{pmatrix}$ which can have zero a-complonent is 0_{2m}. By (2.3) the same can be said about the normal cone in (4.50), and we have $\begin{pmatrix} w_1 \\ \beta_1 \end{pmatrix} = 0_{2m}$, i.e.,

$$-\frac{d}{dt}\begin{pmatrix} Kx + Gr(t) \\ 0 \end{pmatrix} = \begin{pmatrix} w_2 \\ 0 \end{pmatrix} \in \mathcal{U} \times \{0_m\},$$

i.e., we have proven (4.41). It is equivalent to (4.40) and to

$$\dot{x} \in (D_{\xi_0}\varphi)(\operatorname{Ker} R - R^+\dot{r}(t)),$$

which, in turn, means that there is $z \in \operatorname{Ker} R$ such that

$$\dot{x} = (D_{\xi_0}\varphi)(z - R^+\dot{r}(t)). \tag{4.51}$$

Now observe that

$$R(z - R^+\dot{r}(t)) = Rz - RR^+\dot{r}(t) = -\dot{r}(t). \tag{4.52}$$

where the last equality is due to the fact that R^+ is the right inverse of R because of (4.10) and [38, Proposition 2.3]. Write (4.51) and (4.52) together

$$\begin{pmatrix} D_{\xi_0}\varphi \\ R \end{pmatrix}(z - R^+\dot{r}(t)) = \begin{pmatrix} \dot{x} \\ -\dot{r}(t) \end{pmatrix},$$

to observe that

$$\begin{pmatrix} \dot{x} \\ -\dot{r}(t) \end{pmatrix} \in \operatorname{Im} \begin{pmatrix} D_{\xi_0}\varphi \\ R \end{pmatrix}. \tag{4.53}$$

On the other hand, take the time-derivative of (4.28) and apply $\begin{pmatrix} D_{\xi_0}\varphi \\ R \end{pmatrix}$:

$$\begin{pmatrix} D_{\xi_0}\varphi \\ R \end{pmatrix}\dot{\zeta} = \begin{pmatrix} D_{\xi_0}\varphi \\ R \end{pmatrix}\begin{pmatrix} D_{\xi_0}\varphi \\ R \end{pmatrix}^+ \begin{pmatrix} \dot{x} \\ -\dot{r}(t) \end{pmatrix}.$$

Matrix $\begin{pmatrix} D_{\xi_0}\varphi \\ R \end{pmatrix}\begin{pmatrix} D_{\xi_0}\varphi \\ R \end{pmatrix}^+$ is the orthogonal projection matrix onto Im $\begin{pmatrix} D_{\xi_0}\varphi \\ R \end{pmatrix}$ [15, Definition 1.1.2], but, since we already know (4.53), it acts on $\begin{pmatrix} \dot{x} \\ -\dot{r}(t) \end{pmatrix}$ as the identity matrix and we conclude that

$$\begin{pmatrix} D_{\xi_0}\varphi \\ R \end{pmatrix}\dot{\zeta} = \begin{pmatrix} \dot{x} \\ -\dot{r}(t) \end{pmatrix},$$

which, together with (4.29) implies (LSM4) and (LSM5). □

4.3. Implicit catch-up algorithm

One of the common methods to solve a state-dependent sweeping process (4.23) is the implicit catch-up scheme, see, e.g., [16, Theorem 3.3], [52, Section 3.3], and [53]. Specifically, we partition the time interval as

$$0 = t_0 < t_1 < \cdots < t_{k-1} < t_k = T \tag{4.54}$$

and then, for the sweeping process (4.23)-(4.24), on j-th step we are looking for a fixed point of the projection map

$$\begin{pmatrix} \tilde{y} \\ \tilde{a} \end{pmatrix} \mapsto \operatorname{proj}^{\mathbb{K}^{-1}}\left(\begin{pmatrix} y^{j-1} \\ a^{j-1} \end{pmatrix}, C(t_j, \tilde{a})\right), \tag{4.55}$$

and put such a fixed point as $\begin{pmatrix} y^j \\ a^j \end{pmatrix}$ of the discretized solution. Since $C(t, \tilde{a})$ does not depend on $\tilde{y}$, it is enough to find a fixed point of the map

$$\begin{aligned} T_j:\ & \mathbb{R}^m \ \to\ \mathbb{R}^m, \\ T_j:\ & \tilde{a} \ \mapsto\ \begin{pmatrix} 0 & I \end{pmatrix} \operatorname{proj}^{\mathbb{K}^{-1}}\left(\begin{pmatrix} y^{j-1} \\ a^{j-1} \end{pmatrix}, C(t_j, \tilde{a})\right). \end{aligned} \tag{4.56}$$

The standard requirement for the existence for a fixed point is to have the moving set Lipschitz-continuous with Lipschitz constant corresponding to the state variable being strictly less then 1. For our problem we write the conditions of Theorem 1.2 and its counterpart [53, Lemma 2.1, p. 182] for a single time-step:

$$d_H^{\mathbb{K}^{-1}}(C(t_1, \tilde{a}_1), C(t_2, \tilde{a}_2)) \leqslant L_1|t_1 - t_2| + L_2\|\tilde{a}_1 - \tilde{a}_2\|, \qquad L_1, L_2 > 0, \tag{4.57}$$

$$L_2 < 1, \tag{4.58}$$

where $d_H^{\mathbb{K}^{-1}}$ is the Hausdorff distance induced by the norm in the inner product space $\mathcal{V} \times \mathbb{R}^m$:

$$d_H^{\mathbb{K}^{-1}}(C_1, C_2) = \max\left(\sup_{\Sigma_2 \in C_2} \inf_{\Sigma_1 \in C_1} \|\Sigma_1 - \Sigma_2\|_{\mathbb{K}^{-1}}, \sup_{\Sigma_1 \in C_1} \inf_{\Sigma_2 \in C_2} \|\Sigma_1 - \Sigma_2\|_{\mathbb{K}^{-1}}\right) \ \text{ for } C_1, C_2 \subset \mathcal{V} \times \mathbb{R}^m, \tag{4.59}$$

$$\|\Sigma\|_{\mathbb{K}^{-1}} = \sqrt{\Sigma^\top \mathbb{K}^{-1} \Sigma} \qquad \text{for } \Sigma \in \mathcal{V} \times \mathbb{R}^m. \tag{4.60}$$

Remark 4.5. While (4.58) is sufficient for existence of a fixed point, observe from (4.36) that one cannot expect (4.58) to hold when $h_i \geqslant 1$ for some $i \in \overline{1, m}$ (a perfectly plastic spring, or a spring with softening): the points of $C(t, a)$ which correspond to the state of complete failure of spring i will lead to $L_2 \geqslant 1$ (see the "tip" of the set in Figure 4b).

An even stricter (in our setting) assumption would be to require T_j to be a contraction mapping, which would imply both existence and uniqueness of its fixed point. However, as we will demonstrate in Section 5, map T_j in case of softening may not be a contraction even when the state of complete failure is not attained. Examples show that T_j may have multiple fixed points, which means the co-existence of multiple branching solutions of the state-dependent sweeping process (4.23)-(4.24).

Remark 4.6. To find numerically the fixed points of the map T_j at each time-step we iterate the map and hope for convergence to a fixed point, see Algorithm 1 below. However, this means that for each time-step we must make a choice of an initial value for the iterations, and such choice is arbitrary with respect to the given problem data. In Algorithm 1 we denote the choice as a given function $\text{InitialValue}\left(j, a^{j-1}\right)$, and the simplest way to choose is to take the value from the previous time-step, i.e., to set

$$\text{InitialValue}\left(j, a^{j-1}\right) := a^{j-1}.$$

However, as we will illustrate in the next sections, sometimes the map T_j has multiple fixed points simultaneously, and different prescribed choices of InitialValue will result in convergence to different fixed points. This gives the algorithm an advantage over the explicit catch-up method, which also converges [41] under the assumptions, similar to (4.57)-(4.58), but allows no control over the choice of a solution.

But, strictly speaking, Algorithm 1 is searching for *asymptotically stable* fixed points and will fail (diverge) in a situation when T_j has only unstable fixed points, as well as when there are none at all.

4.4. Equivalent sweeping process of reduced dimension

One must note that set $C(t, a)$ is described by time- and state-dependent inequality constraint (Remark 4.4) and a linear equality constraint of $\mathcal{V} \times \mathbb{R}^m \subset \mathbb{R}^{2m}$, which can be explicitly obtained from Proposition 4.1 *i)*. The latter is independent from the arguments of $C(t, a)$, therefore, one can pass to an equivalent state-dependent sweeping process in $\mathbb{R}^{\dim\mathcal{V}+m}$, similarly to the procedure of [38, Section 5.2]. Specifically, we can define set $C_V(t, a)$ such that

$$VC_V(t, a) = C(t, a)$$

by substituting into (4.34)-(4.35) the new unknown variable $\hat{y}(t) \in \mathbb{R}^{\dim\mathcal{V}}$ such that

$$y = V\hat{y}, \qquad \hat{y} = P_V y. \tag{4.61}$$

We obtain the new moving set

$$C_V(t, \tilde{a}) = \left\{ \begin{pmatrix} \hat{y} \\ a \end{pmatrix} \in \mathbb{R}^{\dim\mathcal{V}+m} : \begin{array}{l} \hat{n}_{-i}^\top S_V \begin{pmatrix} \hat{y} - G_V r(t) \\ a - H\tilde{a} \end{pmatrix} - (Ff(t))_i \leqslant c_{0,i}, \\ \hat{n}_{+i}^\top S_V \begin{pmatrix} \hat{y} - G_V r(t) \\ a - H\tilde{a} \end{pmatrix} + (Ff(t))_i \leqslant c_{0,i} \end{array} \text{ for all } i \in \overline{1, m} \right\} \tag{4.62}$$

defined via its normal vectors

$$\hat{n}_{-i} = \begin{pmatrix} -k_i P_V\, e_i \\ -s_i e_i \end{pmatrix} \in \mathbb{R}^{\dim\mathcal{V}+m}, \qquad \hat{n}_{+i} = \begin{pmatrix} k_i P_V\, e_i \\ -s_i e_i \end{pmatrix} \in \mathbb{R}^{\dim\mathcal{V}+m}$$

with respect to the inner product (2.1) in $\mathbb{R}^{\dim \mathcal{V}+m}$ defined via the matrix

$$S_V := \begin{pmatrix} V^\top K^{-1} V & 0 \\ 0 & I \end{pmatrix}.$$

We also denote the matrix

$$G_V := P_V K(D_{\xi_0}\varphi) R^+,$$

compare to (4.20).

Now observe that sweeping process (4.23) can be written as

$$\begin{pmatrix} \dot{y} \\ \dot{a} \end{pmatrix}^\top \mathbb{K}^{-1} \left(\begin{pmatrix} c_y \\ c_a \end{pmatrix} - \begin{pmatrix} y \\ a \end{pmatrix} \right) \geqslant 0 \qquad \text{for any } \begin{pmatrix} c_y \\ c_a \end{pmatrix} \in C(t,a).$$

Using change of variables (4.61) we obtain

$$\left(\begin{pmatrix} V & 0 \\ 0 & I \end{pmatrix} \begin{pmatrix} \dot{\hat{y}} \\ \dot{a} \end{pmatrix} \right)^\top \mathbb{K}^{-1} \begin{pmatrix} V & 0 \\ 0 & I \end{pmatrix} \left(\begin{pmatrix} c_{\hat{y}} \\ c_a \end{pmatrix} - \begin{pmatrix} \hat{y} \\ a \end{pmatrix} \right) \geqslant 0 \qquad \text{for any } \begin{pmatrix} c_{\hat{y}} \\ c_a \end{pmatrix} \in C_V(t,a),$$

which is the sweeping process in $\mathbb{R}^{\dim \mathcal{V}+m}$:

$$-\frac{d}{dt} \begin{pmatrix} \hat{y} \\ a \end{pmatrix} \in N^{S_V}_{C_V(t,a)} \begin{pmatrix} \hat{y} \\ a \end{pmatrix} \tag{4.63}$$

with initial condition

$$\hat{y}(0) = P_V y(0).$$

Given a partition (4.54) we can numerically solve the sweeping process of reduced dimension (4.62)-(4.63) by iterations of

$$\begin{pmatrix} \tilde{\hat{y}} \\ \tilde{a} \end{pmatrix} \mapsto \operatorname{proj}^{S_V} \left(\begin{pmatrix} \hat{y}^{j-1} \\ a^{j-1} \end{pmatrix}, C_V\left(t_j, \tilde{a}\right) \right), \tag{4.64}$$

and Algorithm 2 specifically. Map T_j defined via projection (4.64) coincides with the map as defined by (4.56).

For problems with large m Algorithm 2 is orders of magnitude faster then Algorithm 1 in $\mathbb{R}^{2m}$ for sweeping process (4.23), however the formulation of (4.23), (4.56) is sometimes easier to handle analytically.

Remark 4.7. Observe that the mapping $(k, s, h) \mapsto (k, E^p)$, given by the formula for a plasticity modulus (3.17) is not injective, i.e., for the same values of k and E^p (therefore, for the same observed behavior of a spring), there are many corresponding pairs of values (s, h), which result in such behavior. And, despite the identical observed behavior of the springs, such different pairs of (s, h) lead to significantly different number of iterations of Algorithm 2. In particular, while computing the examples presented further in Section 6 we noticed that equivalent parameters with $s = 1$ require much more iterations per time-step to converge.

Algorithm 1: Iterative numerical scheme to solve the state-dependent sweeping process (4.23)-(4.24).

//Given: $\mathbb{K}$, $C(t,a)$ *by* (4.24), $\begin{pmatrix} y^0 \\ a^0 \end{pmatrix} \in \mathbb{R}^{2m}$ *admissible in the sense of* (4.31),
//a partition t_j, $j \in \overline{0,k}$ *as in* (4.54),
//an initial guess function $\text{InitialValue}\left(j, a^{j-1}\right)$,
//and the constants for the stopping condition:
//very small real $\epsilon > 0$, *large integer* $I_{\max}$, *large real* $R > 0$.
for $j := 1$ **to** k **do**
  $I := 0$;
  converged := **false**;
  diverged := **false**;
  //prescribed at this time-step initial guess for the iterations:
  $a_0^j := \text{InitialValue}\left(j, a^{j-1}\right)$;
  while not (converged **or** diverged) **do**
    $I := I + 1$;
    //An iteration of the map (4.55)*:*
    $\begin{pmatrix} y_I^j \\ a_I^j \end{pmatrix} := \text{proj}^{\mathbb{K}^{-1}}\left(\begin{pmatrix} y^{j-1} \\ a^{j-1} \end{pmatrix}, C\left(t_j, a_{I-1}^j\right)\right)$;
    if $\left\|a_I^j - a_{I-1}^j\right\| < \epsilon$ **then**
      converged := **true**;
    end
    if $I > I_{\max}$ **or** $\left\|\begin{pmatrix} y_I^j \\ a_I^j \end{pmatrix}\right\| > R$ **then**
      //Cannot find an asymptotically stable fixed point of the map T_j *for* j*-th step, its iterations diverge.*
      diverged := **true**;
    end
  end
  if diverged **then**
    break
  end
  $\begin{pmatrix} y^j \\ a^j \end{pmatrix} := \begin{pmatrix} y_I^j \\ a_I^j \end{pmatrix}$;
end

Algorithm 2: Practical iterative numerical scheme to solve the state-dependent sweeping process of reduced dimension (4.62)-(4.63).

//Given S_V, $C_V(t,a)$, $\begin{pmatrix}\hat{y}^0\\ a^0\end{pmatrix} \in \mathbb{R}^{\dim\mathcal{V}+m}$ *such that*
//$\begin{pmatrix}V\hat{y}^0\\ a^0\end{pmatrix}$ *is admissible in the sense of* (4.31)*,*
//a partition t_j, $j \in \overline{0,k}$ *as in* (4.54)*,*
//an initial guess function $\text{InitialValue}\left(j, a^{j-1}\right)$*,*
//and the constants for the stopping condition:
//very small real $\epsilon > 0$*, large integer* $I_{\max}$*, large real* $R > 0$*.*
for $j := 1$ **to** k **do**
  $I := 0$;
  converged := **false**;
  diverged := **false**;
  //initial guess for the iterations, prescribed at this time-step :
  $a_0^j := \text{InitialValue}\left(j, a^{j-1}\right)$;
  while not (converged **or** diverged) **do**
    $I := I + 1$;
    //Iteration of map (4.64)*:*
    $\begin{pmatrix}\hat{y}_I^j\\ a_I^j\end{pmatrix} := \text{proj}^{S_V}\left(\begin{pmatrix}\hat{y}^{j-1}\\ a^{j-1}\end{pmatrix}, C_V\left(t_j, a_{I-1}^j\right)\right)$;
    if $\left\|a_I^j - a_{I-1}^j\right\| < \epsilon$ **then**
      converged := **true**;
    end
    if $I > I_{\max}$ **or** $\left\|\begin{pmatrix}\hat{y}_I^j\\ a_I^j\end{pmatrix}\right\| > R$ **then**
      //Cannot find an asymptotically stable fixed point of the map T_j *for j-th step, its iterations diverge.*
      diverged := **true**;
    end
  end
  if diverged **then**
    break
  end
  $\begin{pmatrix}\hat{y}^j\\ a^j\end{pmatrix} := \begin{pmatrix}\hat{y}_I^j\\ a_I^j\end{pmatrix}$;
end

5. Two-springs system as a toy example with non-unique solutions

As the first example of a lattice, we consider a toy system of two springs connected in series along a line, see Figure 1b. Despite its simplicity, this example can help to illustrate our approach, important properties of the LSMs with softening, behavior of the implicit catch-up algorithm and state-dependent sweeping processes in general.

5.1. Given data

The geometry of the system is represented by the following quantities used in (LSM4)-(LSM5):

$$\begin{aligned}
\text{number of spatial dimensions:} \quad & d = 1,\\
\text{number of nodes:} \quad & n = 3,\\
\text{number of springs:} \quad & m = 2,\\
\text{reference configuration:} \quad & \xi_0 = \begin{pmatrix} 0 & 1 & 2 \end{pmatrix}^\top,\\
\text{incidence matrix:} \quad & Q = \begin{pmatrix} 1 & 0 \\ -1 & 1 \\ 0 & -1 \end{pmatrix}^\top,\\
\text{number of external displacement constraints:} \quad & q = 2,\\
& R = \begin{pmatrix} 1 & 0 & 0 \\ 0 & 0 & 1 \end{pmatrix},\\
\text{displacement load:} \quad & r(t) = \begin{pmatrix} 0 & -l(t) \end{pmatrix}^\top,\\
\text{stress load:} \quad & f(t) = \begin{pmatrix} f_1(t) & f_2(t) & f_3(t) \end{pmatrix}^\top.
\end{aligned}$$

However, we will see, that due to the constraint (LSM5), only the component $f_2(t)$ of $f(t)$ influences the system, see Figure 1b.

As we have $d = 1$, choose the orientation of springs to agree with the positive direction. Then (4.8) yields

$$\begin{aligned}
\text{compatibility matrix:} \quad & D_{\xi_0}\varphi = -Q^\top = \begin{pmatrix} -1 & 1 & 0 \\ 0 & -1 & 1 \end{pmatrix},\\
\text{enhanced compatibility matrix:} \quad & \begin{pmatrix} D_{\xi_0}\varphi \\ R \end{pmatrix} = \begin{pmatrix} -1 & 1 & 0 \\ 0 & -1 & 1 \\ 1 & 0 & 0 \\ 0 & 0 & 1 \end{pmatrix}.
\end{aligned}$$

Assumptions (4.10) and (4.11) are satisfied trivially. We compute (see (4.13))

$$F_1 = \frac{1}{4}\begin{pmatrix} -1 & 2 & 1 \\ -1 & -2 & 1 \end{pmatrix}.$$

At this point we leave the parameters of the springs arbitrary, i.e., we suppose to be given

$$\begin{aligned} \text{Hooke's coefficients:} &\quad k_1, k_2 > 0, \\ \text{coefficients of state-dependent feedback:} &\quad h_1, h_2 \in \mathbb{R}, \\ \text{geometric slopes:} &\quad s_1, s_2 > 0, \\ \text{initial yield stresses:} &\quad c_{0,1}, c_{0,2} > 0. \end{aligned} \tag{5.1}$$

Thus, we have

$$K = \begin{pmatrix} k_1 & 0 \\ 0 & k_2 \end{pmatrix}, \qquad H = \begin{pmatrix} h_1 & 0 \\ 0 & h_2 \end{pmatrix}.$$

5.2. The sweeping process

Observe that

$$\operatorname{Ker} R = \operatorname{lin} \begin{pmatrix} 0 & 1 & 0 \end{pmatrix}^\top,$$

therefore, from (4.17) we have

$$\mathcal{V}^\perp = (D_{\xi_0}\varphi) \operatorname{Ker} R = \operatorname{lin} \begin{pmatrix} -1 & 1 & 0 \\ 0 & -1 & 1 \end{pmatrix} \begin{pmatrix} 0 \\ 1 \\ 0 \end{pmatrix} = \operatorname{lin} \begin{pmatrix} 1 \\ -1 \end{pmatrix}$$

and from (4.14) we have

$$U = \begin{pmatrix} k_1 \\ -k_2 \end{pmatrix}, \qquad \mathcal{U} = \operatorname{Im} U.$$

Moreover,

$$\mathcal{V} = \operatorname{lin} \begin{pmatrix} 1 \\ 1 \end{pmatrix},$$

but for future convenience we would like to have matrix V such that

$$V^\top K^{-1} V = I,$$

where I in our case is $I_{1\times 1} = 1$. Thus, if we take

$$V = \kappa \begin{pmatrix} 1 \\ 1 \end{pmatrix} \tag{5.2}$$

for some $\kappa > 0$ and solve

$$\begin{aligned} \kappa \begin{pmatrix} 1 & 1 \end{pmatrix} \begin{pmatrix} k_1^{-1} & 0 \\ 0 & k_2^{-1} \end{pmatrix} \begin{pmatrix} 1 \\ 1 \end{pmatrix} \kappa &= 1, \\ \kappa^2 (k_1^{-1} + k_2^{-1}) &= 1, \\ \kappa &= \frac{1}{\sqrt{k_1^{-1} + k_2^{-1}}}, \end{aligned} \tag{5.3}$$

so we have the basis vector of $\mathcal{V}$ as (5.2)-(5.3).

Furthermore, by (4.19)

$$P_U = \left(U^\top K^{-1} U\right)^{-1} U^\top K^{-1} = \frac{1}{k_1 + k_2}\begin{pmatrix} 1 & -1 \end{pmatrix},$$
$$P_V = \left(V^\top K^{-1} V\right)^{-1} V^\top K^{-1} = I\, V^\top K^{-1} = \kappa\begin{pmatrix} 1 & 1 \end{pmatrix}\begin{pmatrix} k_1^{-1} & 0 \\ 0 & k_2^{-1} \end{pmatrix} = \kappa\begin{pmatrix} k_1^{-1} & k_2^{-1} \end{pmatrix},$$

and

$$UP_U = \frac{1}{k_1 + k_2}\begin{pmatrix} k_1 & -k_1 \\ -k_2 & k_2 \end{pmatrix},$$
$$VP_V = \kappa^2\begin{pmatrix} 1 \\ 1 \end{pmatrix}\begin{pmatrix} k_1^{-1} & k_2^{-1} \end{pmatrix} = \kappa^2\begin{pmatrix} k_1^{-1} & k_2^{-1} \\ k_1^{-1} & k_2^{-1} \end{pmatrix}.$$

Finally,

$$F = UP_U F_1 = \frac{1}{k_1 + k_2}\begin{pmatrix} 0 & k_1 & 0 \\ 0 & -k_2 & 0 \end{pmatrix},$$
$$R^+ = R^\top (RR^\top)^{-1} = \begin{pmatrix} 1 & 0 \\ 0 & 0 \\ 0 & 1 \end{pmatrix}\begin{pmatrix} 1 & 0 \\ 0 & 1 \end{pmatrix}^{-1} = \begin{pmatrix} 1 & 0 \\ 0 & 0 \\ 0 & 1 \end{pmatrix},$$

$$\begin{aligned} G_V\, r(t) &= P_V K(D_{\xi_0}\varphi) R^+ r(t) \\ &= \kappa\begin{pmatrix} k_1^{-1} & k_2^{-1} \end{pmatrix}\begin{pmatrix} k_1 & 0 \\ 0 & k_2 \end{pmatrix}\begin{pmatrix} -1 & 1 & 0 \\ 0 & -1 & 1 \end{pmatrix}\begin{pmatrix} 1 & 0 \\ 0 & 0 \\ 0 & 1 \end{pmatrix}\begin{pmatrix} 0 \\ -l(t) \end{pmatrix} \\ &= \kappa\begin{pmatrix} 1 & 1 \end{pmatrix}\begin{pmatrix} -1 & 0 \\ 0 & 1 \end{pmatrix}\begin{pmatrix} 0 \\ -l(t) \end{pmatrix} = -\kappa l(t), \\ Gr(t) &= VG_V\, r(t) = -\kappa^2\begin{pmatrix} 1 \\ 1 \end{pmatrix} l(t), \\ Ff(t) &= \begin{pmatrix} k_1 \\ -k_2 \end{pmatrix}\frac{f_2(t)}{k_1 + k_2}. \end{aligned}$$

Therefore, we have sweeping process (4.23) in $\mathbb{R}^4$ where

$$\mathbb{K}^{-1} = \begin{pmatrix} k_1^{-1} & 0 & 0 & 0 \\ 0 & k_2^{-1} & 0 & 0 \\ 0 & 0 & 1 & 0 \\ 0 & 0 & 0 & 1 \end{pmatrix},$$

and, by (4.34)-(4.35),

$$n_{-1} = \begin{pmatrix} -\kappa^2 \\ -\kappa^2 \\ -s_1 \\ 0 \end{pmatrix}, \quad n_{-2} = \begin{pmatrix} -\kappa^2 \\ -\kappa^2 \\ 0 \\ -s_2 \end{pmatrix}, \quad n_{+1} = \begin{pmatrix} \kappa^2 \\ \kappa^2 \\ -s_1 \\ 0 \end{pmatrix}, \quad n_{+2} = \begin{pmatrix} \kappa^2 \\ \kappa^2 \\ 0 \\ -s_2 \end{pmatrix},$$

$$C\left(t,\begin{pmatrix}\tilde{a}_1\\ \tilde{a}_2\end{pmatrix}\right)=\left\{\begin{pmatrix}y_1\\ y_2\\ a_1\\ a_2\end{pmatrix}\in\mathbb{R}^4 : y_1=y_2,\ \begin{pmatrix}n_{-1}^\top\\ n_{-2}^\top\\ n_{+1}^\top\\ n_{+2}^\top\end{pmatrix}\mathbb{K}^{-1}\begin{pmatrix}y_1+\kappa^2 l(t)\\ y_2+\kappa^2 l(t)\\ a_1-h_1\tilde{a}_1\\ a_2-h_2\tilde{a}_2\end{pmatrix}+\begin{pmatrix}-k_1\\ k_2\\ k_1\\ -k_2\end{pmatrix}\frac{f_2(t)}{k_1+k_2}\leqslant\begin{pmatrix}c_{0,1}\\ c_{0,2}\\ c_{0,1}\\ c_{0,2}\end{pmatrix}\right\},$$

where the inequality is meant in the component-wise sense.

Equivalent sweeping process (4.63) in $\mathbb{R}^3$ is defined via

$$S_V = I_{3\times 3}$$

and

$$\hat{n}_{-1}=\begin{pmatrix}-\kappa\\ -s_1\\ 0\end{pmatrix},\ \hat{n}_{-2}=\begin{pmatrix}-\kappa\\ 0\\ -s_2\end{pmatrix},\ \hat{n}_{+1}=\begin{pmatrix}\kappa\\ -s_1\\ 0\end{pmatrix},\ \hat{n}_{+2}=\begin{pmatrix}\kappa\\ 0\\ -s_2\end{pmatrix}, \tag{5.4}$$

$$C_V\left(t,\begin{pmatrix}\tilde{a}_1\\ \tilde{a}_2\end{pmatrix}\right)=\left\{\begin{pmatrix}\hat{y}\\ a_1\\ a_2\end{pmatrix}\in\mathbb{R}^3 : \begin{pmatrix}\hat{n}_{-1}^\top\\ \hat{n}_{-2}^\top\\ \hat{n}_{+1}^\top\\ \hat{n}_{+2}^\top\end{pmatrix}\begin{pmatrix}\hat{y}+\kappa\, l(t)\\ a_1-h_1\tilde{a}_1\\ a_2-h_2\tilde{a}_2\end{pmatrix}+\begin{pmatrix}-k_1\\ k_2\\ k_1\\ -k_2\end{pmatrix}\frac{f_2(t)}{k_1+k_2}\leqslant\begin{pmatrix}c_{0,1}\\ c_{0,2}\\ c_{0,1}\\ c_{0,2}\end{pmatrix}\right\}. \tag{5.5}$$

5.3. Non-uniqueness of solutions and a bifurcation

Consider the sweeping process (4.63), (5.4) and (5.5) on an interval $[t_0, T]$. Let $l(t)$ be Lipschitz-continuous and monotonically increasing from zero, and f be zero:

$$\dot{l}(t) > 0, \quad f(t)\equiv 0 \quad \text{a.e. on } [t_0,T], \qquad l(t_0)=0. \tag{5.6}$$

Choose an initial condition $\begin{pmatrix}\hat{y}(t_0)\\ a(t_0)\end{pmatrix}\in\mathbb{R}^3$ on the boundary of $C_V(t,a)$ corresponding to both normal vectors $\hat{n}_{+1}, \hat{n}_{+2}$ being active, i.e., in terms of (4.39) for $t=t_0$ we must have both

$$g_{+1}\left(t,a(t),\begin{pmatrix}V\hat{y}(t)\\ a(t)\end{pmatrix}\right)=0, \qquad g_{+2}\left(t,a(t),\begin{pmatrix}V\hat{y}(t)\\ a(t)\end{pmatrix}\right)=0. \tag{5.7}$$

Additionally, we require that the constraints with normal vectors $\hat{n}_{-1}, \hat{n}_{-2}$ are not active at the initial condition, i.e., for $t=t_0$:

$$g_{-1}\left(t,a(t),\begin{pmatrix}V\hat{y}(t)\\ a(t)\end{pmatrix}\right)<0, \qquad g_{-2}\left(t,a(t),\begin{pmatrix}V\hat{y}(t)\\ a(t)\end{pmatrix}\right)<0. \tag{5.8}$$

In other words we require the stresses of both springs to start at the upper threshold and *not* at the state of complete failure.

We consider three scenarios: *A.* both springs are hardening springs ($h_1, h_2 < 1$), *B.* both springs are perfectly plastic ($h_1 = h_2 = 1$) and *C.* both springs are softening springs ($h_1, h_2 > 1$).

Proposition 5.1. *Given the sweeping process* (4.63), (5.4) *and* (5.5) *on an interval* $[t_0, T]$ *and assuming* (5.6)–(5.8) *the following solutions are present, as long as* (5.8) *holds:*

A) If both $h_1, h_2 < 1$ then there is a single soluton with plastic deformation distributed between both springs, and it is given by

$$\begin{pmatrix} \dot{\hat{y}} \\ \dot{a}_1 \\ \dot{a}_2 \end{pmatrix} = -\frac{(1-h_2)s_2^2\,\hat{n}_{+1} + (1-h_1)s_1^2\,\hat{n}_{+2}}{(1-h_1)s_1^2 + (1-h_2)s_2^2 + (k_1^{-1}+k_2^{-1})(1-h_1)(1-h_2)s_1^2 s_2^2}\dot{l}(t) \tag{5.9}$$

for a.a. $t \geqslant t_0$.

B) If $h_1 = h_2 = 1$ then there is a continuum of solutions branching at t_0 and with derivatives

$$\begin{pmatrix} \dot{\hat{y}} \\ \dot{a}_1 \\ \dot{a}_2 \end{pmatrix} \in \left\{ -\left(\theta\,\hat{n}_{+1} + (1-\theta)\hat{n}_{+2}\right)\dot{l}(t) : \theta \in [0,1] \right\}.$$

C) If both $h_1, h_2 > 1$ then there may be up to three solutions branching at t_0, namely:

1) Plastic deformation becomes localized in spring 1:

$$\begin{pmatrix} \dot{\hat{y}} \\ \dot{a}_1 \\ \dot{a}_2 \end{pmatrix} = -\frac{1}{1 + (k_1^{-1}+k_2^{-1})(1-h_1)s_1^2}\,\dot{l}(t)\,\hat{n}_{+1}, \quad \textit{possible iff} \quad (k_1^{-1}+k_2^{-1})(1-h_1)s_1^2 > -1.$$

2) Plastic deformation becomes localized in spring 2:

$$\begin{pmatrix} \dot{\hat{y}} \\ \dot{a}_1 \\ \dot{a}_2 \end{pmatrix} = -\frac{1}{1 + (k_1^{-1}+k_2^{-1})(1-h_2)s_2^2}\,\dot{l}(t)\,\hat{n}_{+2}, \quad \textit{possible iff} \quad (k_1^{-1}+k_2^{-1})(1-h_2)s_2^2 > -1.$$

3) Distributed solution (5.9)*, which is possible iff*

$$(1-h_1)s_1^2 + (1-h_2)s_2^2 + (k_1^{-1}+k_2^{-1})(1-h_1)(1-h_2)s_1^2 s_2^2 < 0. \tag{5.10}$$

We must note, that because any point t along the solution (5.9) satisfies (5.7), in the case *C)* there technically is a continuum of solutions, with branching from (5.9) at every $t \geqslant t_0$. Also, note that our conclusions in the case *C)* agree with the conclusions of [17].

Proof of Proposition 5.1. To save space we will omit complete derivations, as they are straightforward, yet cumbersome and very similar to the proof of Proposition 3.1. The following applies to a.a. $t \in [t_0, T]$. At first, we consider the case of the solution driven by the facet of C_V with the normal vector $\hat{n}_{+1}$, i.e., we must find the unknown quantities $\dot{\hat{y}}, \dot{a}_1, \dot{a}_2 \in \mathbb{R}$ such that

$$\hat{n}_{+1}^{\top} \begin{pmatrix} \dot{\hat{y}} + \kappa\,\dot{l}(t) \\ (1-h_1)\dot{a}_1 \\ (1-h_2)\dot{a}_2 \end{pmatrix} = 0,$$

$$-\begin{pmatrix} \dot{\hat{y}} \\ \dot{a}_1 \\ \dot{a}_2 \end{pmatrix} = \hat{n}_{+1}\,\lambda, \qquad \text{for some } \lambda \geqslant 0,$$

yet such solution must not violate the constraint with $\hat{n}_{+1}$ in order to stay in the moving set C_V:

$$\hat{n}_{+2}^{\top}\begin{pmatrix}\dot{\hat{y}}+\kappa\,\dot{l}(t)\\(1-h_1)\dot{a}_1\\(1-h_2)\dot{a}_2\end{pmatrix}\leqslant 0. \tag{5.11}$$

By manually solving the equations we arrive to the localized solution 1) and its associated condition, present in the case *C)*. It is also present in the case *B)*, as a member of the family of solutions with $\theta = 1$, but (5.11) plays a role and excludes such solution when $h_1 < 1$.

Similarly, by manually solving

$$\hat{n}_{+2}^{\top}\begin{pmatrix}\dot{\hat{y}}+\kappa\,\dot{l}(t)\\(1-h_1)\dot{a}_1\\(1-h_2)\dot{a}_2\end{pmatrix}=0,$$

$$-\begin{pmatrix}\dot{\hat{y}}\\\dot{a}_1\\\dot{a}_2\end{pmatrix}=\hat{n}_{+2}\,\lambda,\qquad \text{for some } \lambda\geqslant 0,$$

and checking that

$$\hat{n}_{+1}^{\top}\begin{pmatrix}\dot{\hat{y}}+\kappa\,\dot{l}(t)\\(1-h_1)\dot{a}_1\\(1-h_2)\dot{a}_2\end{pmatrix}\leqslant 0,$$

we deduce that in the case *C)* the localized solution 2) is present, and also we have it in the case *B)* as a member of the family of solutions with $\theta = 0$.

Finally, by solving

$$\hat{n}_{+1}^{\top}\begin{pmatrix}\dot{\hat{y}}+\kappa\,\dot{l}(t)\\(1-h_1)\dot{a}_1\\(1-h_2)\dot{a}_2\end{pmatrix}=0,\qquad \hat{n}_{+2}^{\top}\begin{pmatrix}\dot{\hat{y}}+\kappa\,\dot{l}(t)\\(1-h_1)\dot{a}_1\\(1-h_2)\dot{a}_2\end{pmatrix}=0,$$

$$-\begin{pmatrix}\dot{\hat{y}}\\\dot{a}_1\\\dot{a}_2\end{pmatrix}=\hat{n}_{+1}\,\lambda_1+\hat{n}_{+2}\,\lambda_2\qquad \text{for some } \lambda_1,\lambda_2\geqslant 0,$$

and carefully treating all the possibilities we arrive to the conclusions of the cases *A)*, *B)*, and the distributed solution 3) in the case *C)*. □

It is, of course, possible to complete the statement of Proposition 5.1 with the cases, where the springs do not have the same type of plasticity, but such study is beyond our current goal of merely showing non-unique solutions emerging via the nonsmooth bifurcation.

By using the numerical implicit catch-up scheme we can immediately observe additional properties of the solutions, namely, their *stability* is the sense of the stability of the corresponding fixed point of the map T_j. Specifically, we take

$$k_1 = k_2 = 1,\qquad s_1 = s_2 = 1,\qquad c_{0,1} = c_{0,2} = 0.01,$$

initial condition

$$\sigma_1(0) = \sigma_2(0) = 0.01, \qquad a_1(0) = a_2(0) = 0, \qquad p_1(0) = p_2(0) = 0,$$

and in Figure 8 we plot mapping T_j, where $j = 1, t_0 = 0, t_1 = 0.0004$. We examine the cases of h as in Proposition 5.1. From Figure 8 we make the following Observation 5.1.

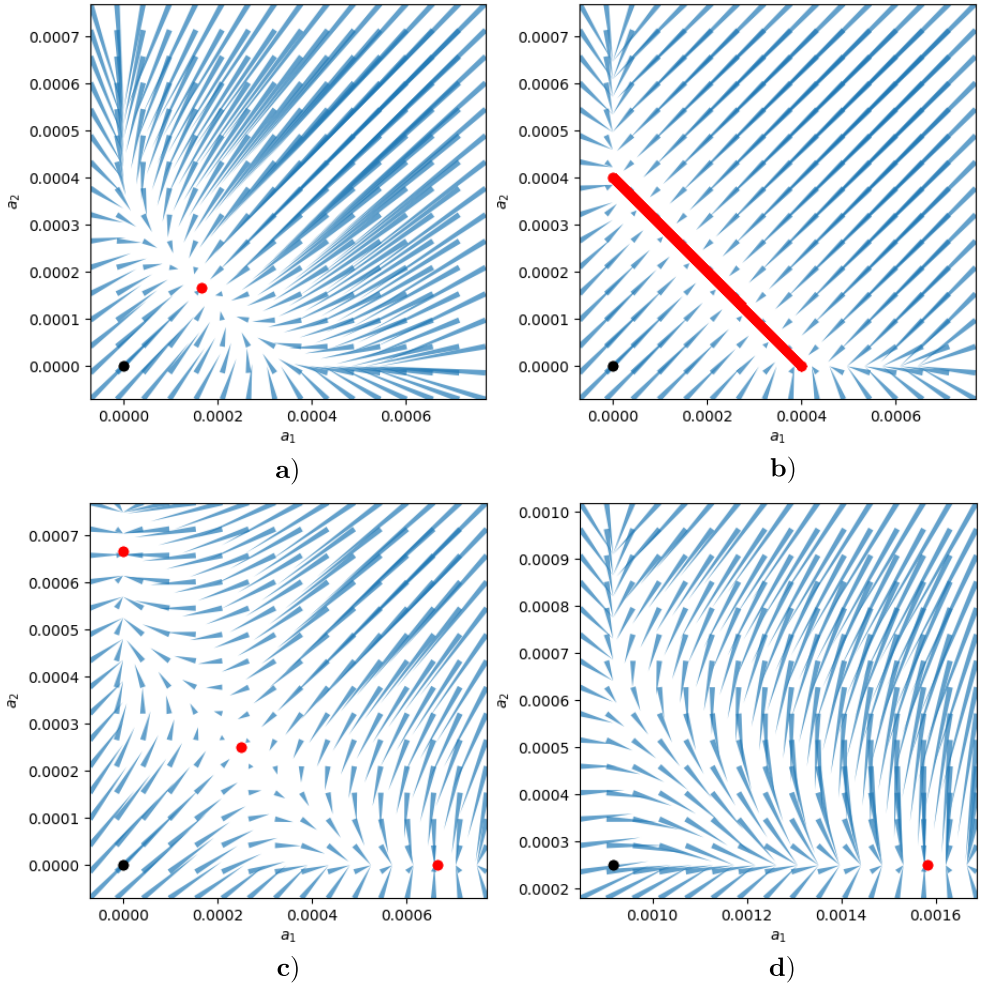

Figure 8. Chart of mapping T_j in the implicit catch-up scheme for the two-springs system. The projected value of a (i.e., a^{j-1} in terms of (4.56)) is shown as the black point, while the red points represent the fixed points a^j of T_j. Each wedge connects a sample value a and the corresponding value $T_j a$. a) Case of hardening $h_1 = h_2 = 0.8$. b) Case of perfect plasticity $h_1 = h_2 = 1$. c) Case of softening $h_1 = h_2 = 1.2$ with a^{j-1} satisfying (5.7), i.e., belonging to the distributed solution *3)* from Proposition 5.1. Observe the saddle fixed point with its stable and unstable sets. d) Case of softening $h_1 = h_2 = 1.2$ with a^{j-1} satisfying only the first equation of (5.7), i.e., belonging to the localized solution *1)* from Proposition 5.1.

Observation 5.1. Consider map T_j as (4.56) for the two-springs system such that $\begin{pmatrix} y^{j-1} \\ a^{j-1} \end{pmatrix}$ satisfies (5.7)-(5.8). From the numerical results presented in Figure 8 we conclude that T_j undergoes a bifurcation when $h_1 = h_2$ go through value 1. Specifically, we see that:

A) In the case of hardening T_j has a single fixed point (Figure 8a), which is stable is the sense of iterations of T_j and which corresponds to the unique solution of Proposition 5.1 *A)*.

B) In the case of perfect plasticity T_j has an interval of fixed points, which is an attracting set for the iterations of T_j (Figure 8b). This agrees with Proposition 5.1 *B)*.

C) In case of softening and a_j satisfying (5.7) the mapping T_j has three fixed points (Figure 8c), two of which are stable and they correspond to the localized solutions *1)* and *2)* of Proposition 5.1. The third fixed point is of the saddle type and it corresponds to the distributed solution *3)*. However,

(a) If for the next time-step $j' = j + 1$ the projected point $a^{j'-1}$ is taken as the saddle fixed point (i.e., the numerical solution follows *3)*), then $T_{j'}$ will again have three fixed points of the same types.

(b) If for the next time-step $j' = j + 1$ the projected point $a^{j'-1}$ is taken as one of the stable fixed points (i.e., the numerical solution follows *1)* or *2)*) then $T_{j'}$ will have only one stable fixed point (Figure 8d), corresponding to the continuation of the branched localized solution.

Remark 5.1. We note that bifurcation with the birth of two additional fixed points and the change of stability in the existing fixed point is similar to the classical pitchfork bifurcation (see, e.g., [78, Figures 3.4.2 and 8.1.6]). However, the map T_j is nonsmooth, therefore, the classical analysis of bifurcations via the eigenvalues of its linearization is not applicable.

Finally, recall Remark 4.6 and observe from Figure 8b,c, how different choices of the initial guess InitialValue(j, a^{j-1}) in Algorithms 1 and 2 can lead to different fixed points found numerically in this example.

5.4. Non-contractiveness of the iterated map near the saddle point due to coupling of springs

The following question arises naturally:

Question. *From both analytical (Proposition 5.1) and numerical (Figure 8) evidence we deduce that in the case of softening there can be three branching solutions when $k_1, k_2 > 0$ are fixed and $s_1, s_2 > 0$ are not too large. However, for individual (uncoupled) springs, by taking smaller and smaller $s > 0$ we can make the Lipschitz constant of the map $\tilde{a} \mapsto \mathrm{proj}^{\mathbb{K}^{-1}}(\Sigma, C(t, \tilde{a}))$ arbitrarily small for a general $\Sigma \in \mathbb{R}^2$, unless the projection goes to the point of complete failure. One can observe this from Figures 4c and 7a, where the boundary of $C(t, \tilde{a})$ would approach the vertical line as $s > 0$ decreases. Now, in the case of two coupled springs, why it is not possible to choose s_1, s_2 small enough to make map T_j a contraction?*

To answer this question we sketch the moving set $C_V(t, a)$ of the sweeping process (4.63), which, in case of the two-springs system, is a subset of $\mathbb{R}^3$ given by (5.4)-(5.5), see Figure 9.

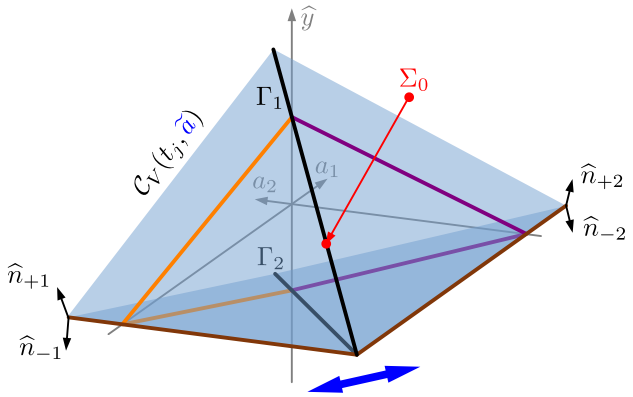

Figure 9. Moving set $C_V(t, a)$ of the sweeping process (5.4)-(5.5), corresponding to the two-springs system and (shown in red) a projection of a point Σ_0 onto the set (i.e., map (4.64) for $\Sigma_0 = \begin{pmatrix} \hat{y}^{j-1} \\ a^{j-1} \end{pmatrix}$). Set C_V is a representation of C in coordinates of a three-dimensional subspace $\mathcal{V} \times \mathbb{R}^2 \subset \mathbb{R}^4$. Brown edges are the states of complete failure. Orange and purple angles show the coupled constraints of springs 1 and 2, respectively (one can see them as two instances of constraints of Figure 4b. By Γ_1 and Γ_2 we denote the "diagonal" edges, shown in black. Blue arrow indicates the direction along to the unstable set of the saddle fixed point in Figure 8c.

From Figure 9 we can provide a visual geometric answer to the question. The following is not a formal proof, but rather an observation from Figures 8c and 9. However, we still think that it is a valuable explanation of how *coupling* of two spings can lead to non-contracting map T_j and, therefore, multiple solutions.

Observe, that no matter how small we take $s_1, s_2 > 0$ (i.e., no matter how pointed are the orange and purple angles, similar to the angle in Figure 4b, the edges Γ_1, Γ_2 are still present. Let $h_1, h_2 > 1$ satisfy (5.10), a projected point $\Sigma_0 = \begin{pmatrix} \hat{y}^{j-1} \\ a^{j-1} \end{pmatrix}$ satisfy (5.7)-(5.8), which means that T_j has a saddle fixed point a^*, see Figure 8c. Then the projection

$$\begin{pmatrix} \hat{y}^* \\ a^* \end{pmatrix} := \text{proj}\left(\Sigma_0, C_V\left(t_j, a^*\right)\right) \tag{5.12}$$

lays exactly on edge Γ_1, as shown in Figure 9.

A small perturbation $\Delta \in \mathbb{R}^2$ of a^* translates the moving set by the vector $\begin{pmatrix} 0 \\ H\Delta \end{pmatrix}$. Take Δ such that $\begin{pmatrix} 0 \\ H\Delta \end{pmatrix}$ is parallel to the blue direction in Figure 9, i.e., it is parallel to the unstable set of the saddle point in Figure 8c. When the magnitude of Δ is small enough, the projection

$$\begin{pmatrix} \hat{y}_\Delta \\ a_\Delta \end{pmatrix} := \text{proj}\left(\Sigma_0, C_V\left(t_j, a^* + \Delta\right)\right) = \text{proj}\left(\Sigma_0, C_V\left(t_j, a^*\right) + \begin{pmatrix} 0 \\ H\Delta \end{pmatrix}\right)$$

will remain on the edge Γ_1, which is translated together with the whole set by $\begin{pmatrix} 0 \\ H\Delta \end{pmatrix}$.

Projection (5.12) means that

$$\Sigma_0 - \begin{pmatrix} \hat{y}^* \\ a^* \end{pmatrix} \in N_{C_V(t_j,a^*)}\left(\begin{pmatrix} \hat{y}^* \\ a^* \end{pmatrix}\right), \tag{5.13}$$

where the normal cone in the right-hand side becomes very narrow for small $s_1, s_2 > 0$. This can be observed from Figure 9 as the entire set $C_V(t_j, a^*)$ would become "flatter" and closer to the plane a_1,a_2. The narrow normal cone means that $\Sigma_0 - \begin{pmatrix} \hat{y}^* \\ a^* \end{pmatrix}$ (parallel to the red vector in Figure 9) is nearly orthogonal to $\begin{pmatrix} 0 \\ H\Delta \end{pmatrix}$ (parallel to the blue diection). Therefore, for $H\Delta$ of small magnitudes

$$\begin{pmatrix} \hat{y}_\Delta \\ a_\Delta \end{pmatrix} - \begin{pmatrix} \hat{y}^* \\ a^* \end{pmatrix} \approx \begin{pmatrix} 0 \\ H\Delta \end{pmatrix},$$

i.e.,

$$T_j(a^* + \Delta) - T_j(a^*) = a_\Delta - a^* \approx H\Delta.$$

Since we had $h_1, h_2 > 1$, we cannot make T_j to be a contraction mapping, no matter how small we take $s_1, s_2 > 0$. Notice, that the slopes, controlled by s_1, s_2 (orange and purple in Figure 9) will essentially affect a_Δ only when Δ is large enough for the projection $\begin{pmatrix} \hat{y}_\Delta \\ a_\Delta \end{pmatrix}$ to no longer lay on the edge Γ_1, however, the "large enough" itself depends on how narrow is the normal cone in (5.13), which, in turn, depends on s_1, s_2.

6. Numerical results for regular lattices: strain localization into a shear band

We apply Algorithm 2 to solve for the evolution in regular lattices and lattices with defects.

6.1. Rectangular lattice

Consider a two-dimensional rectangular lattice of 10×15 nodes spaced with the horizontal and vertical step of 0.5, see Figure 10a. Apply the following boundary condition: all the nodes in the lowest row have their y-coordinate restrained to 0 and all the nodes in the uppermost row have their y-coordinate restrained to a value, which monotonically increases with time. We also restrain the x-coordinate of a single node to a constant value in order to achieve kinematic determinacy (Assumption 2). The following values characterize the lattice:

number of spatial dimensions:	$d = 2$,
number of nodes:	$n = 150$,
number of springs:	$m = 527$,
number of external displacement constraints:	$q = 21$,
dimension of the space of self-stresses:	$\dim \mathcal{V} = 248$.

We will consider several cases.

6.1.1. Symmetric lattice with softening

See Figure 10, where all of the springs have the following parameters:

$$k_i = 1, \quad h_i = 1.1, \quad s_i = 0.3, \quad c_{0,i} = 0.01, \qquad i \in \overline{1,m}. \tag{6.1}$$

We would like to illustrate the evolution of the damage variable a (Figure 10a–d), which is connected to plastic deformation, and the evolution of stress σ (Figure 10e,f). Additionally, Figure 10i shows the number of iterations of map T_j (see (4.56) and (4.64)) required for convergence at each time-step of Algorithm 2. Finally, Figure 10j shows the total stress of the lattice along the vertical direction, which we compute as

$$\sigma^{22}_{total} = \frac{1}{A} \sum_{i \in \overline{1,m}} (\sigma_i \mathcal{D}_{i2}) \left((\varphi(\xi_0))_i \mathcal{D}_{i2} \right), \tag{6.2}$$

where the constant $A = (15-1)(10-1) = 126$ is the area of the lattice in the reference configuration ξ_0, function φ is given by (4.7), and matrix $\mathcal{D}$ is given by (4.9). For details on formula (6.2) we refer to [38, Section 7.2], [54, (6)], [70, (1.2)], and [87, p. 6].

During the evolution of the symmetric rectangular lattice with softening from the relaxed reference configuration (Figure 10a we observe the elastic phase, followed by the accumulation of symmetrically distributed plastic deformation. The symmetric plastic phase happens from $t = 1.36$ to $t = 2.78$, and it can be distinguished on the graph of the number of iterations (Figure 10i) and on the graph of total stress (Figure 10j). At $t = 2.78$ we observe a sudden loss of symmetry of the solution and the beginning of strain localization into the diagonal shear band (Figure 10b,c,f,g). This corresponds to the sharp peak in the number of iterations and to the maximal total stress. All further deformation will happen in the shear band, and its elements remain in the plastic regime with softening, while the rest of the lattice unloads elastically (Figure 10h). This way, the total stress decreases linearly with the increasing displacement load after $t = 2.78$ (Figure 10j), eventually leading to the state of complete failure.

Notice, that we have obtained a non-symmetric solution in a symmetric problem, which suggests non-uniqueness of solutions. And, indeed, by modyfing the initial guess during the loss of symmetry (for t near 2.78, cf. Remark 4.6 on InitialValue) we are able to obtain another solution, in which the shear band develops in the opposite direction (see Figure 3).

We also expect that there may be symmetric solutions to the problem, which are numerically unstable, similarly to the situation in the toy system, see Figure 8c and Observation 5.1 *C)*.

Full videos and computer programs of numerical simulations of this and other examples are included as a supplemental material [79].

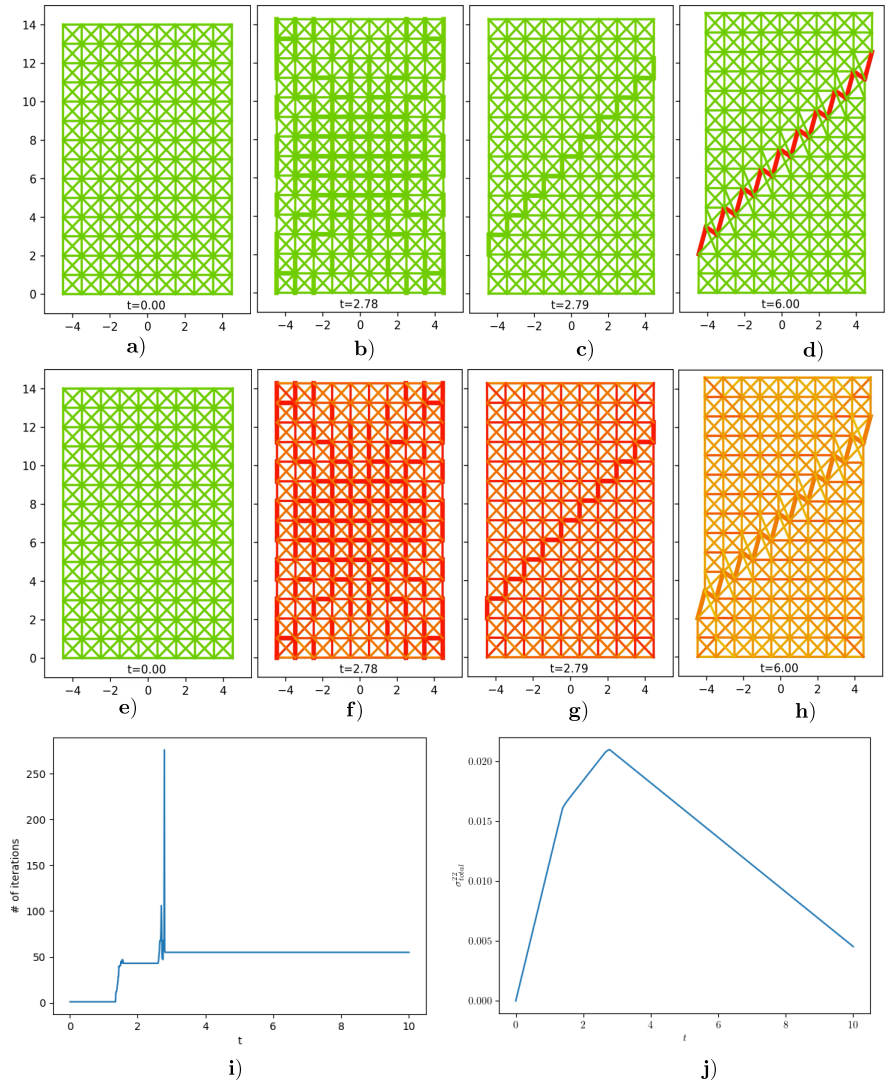

Figure 10. Evolution of a **symmetric** rectangular lattice with **softening** under increasing displacement load along the vertical axis (see Section 6.1.1). a)–d) Thicker lines denote the springs in the plastic regime, and color denotes the value of the damage variable a (green= 0, red = $\max_{t\in[0,6]} a_i(t)$). e)–h) Thicker lines denote the springs in the plastic regime, and color denotes the absolute value of the stress σ (green= 0, yellow=an intermediate value, red = $\max_{t\in[0,6]} |\sigma_i(t)|$). i) the number of iterations of map (4.64) for each time-step. j) total stress (6.2) of the lattice in the vertical direction.

6.1.2. Lattice with a defect with softening

See Figure 11, where all of the springs have the same parameters (6.1), but we introduce a geometric defect into the lattice to destroy its symmetry. We observe essentially the same behavior as in the case of symmetric lattice with softening, but the diagonal shear band now forms to include the location of the defect. It is also accompanied by the minor shear band, formed in the opposite direction (see Figure 11g and the supplemental material [79]). The dissolution of the minor shear band at $t = 3.61$ is

marked by another peak in the number of iterations (see Figure 11i) and a small, but noticable change of the total plasticity modulus of the lattice (see Figure 11j).

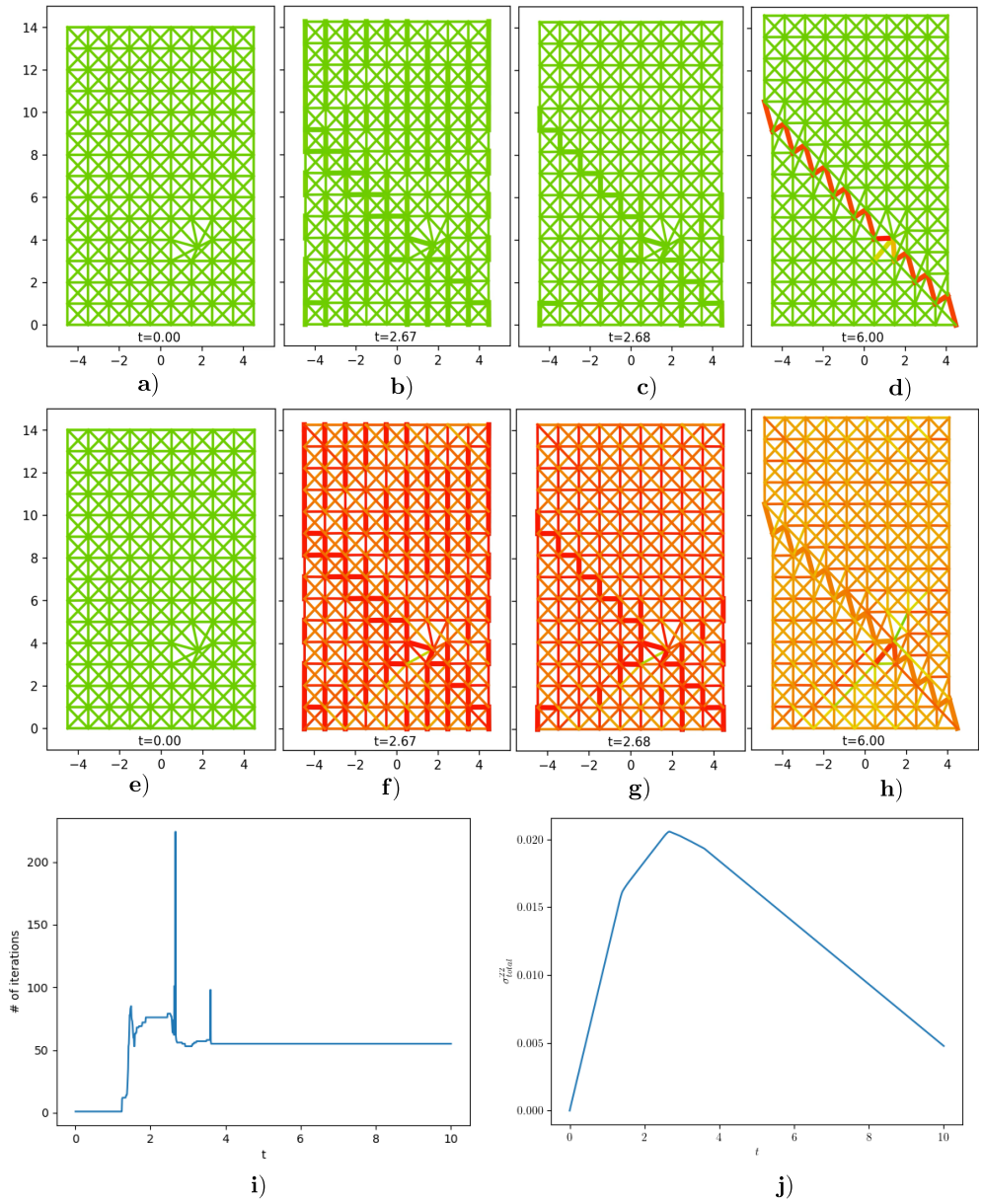

Figure 11. Evolution of a rectangular lattice with a **defect** with **softening** under increasing displacement load along the vertical axis (see Section 6.1.2). The presentation is similar to Figure 10.

6.1.3. Symmetric lattice with perfect plasticity

See Figure 12, where all of the springs have the following parameters:

$$k_i = 1, \quad h_i = 1, \quad s_i = 0.3, \quad c_{0,i} = 0.01, \qquad i \in \overline{1,m}. \tag{6.3}$$

Notice, that no localization is present, and the deformation, as well as stress, is symmetrically distributed in the lattice. We know that the evolution of stresses is unique for elastic-perfectly plastic lattices [38, Theorems 4.1 and 5.1], as well as for elastic-perfectly plastic bodies in general. We do not exclude the possibility that there could be other solutions to the problem with the same trajectory of the stress variable (Figure 12e–h,j), but different trajectories of the damage variable (Figure 12a–d), and, therefore, different displacements. However, at the moment we were not able to find such alternative solutions in the current example.

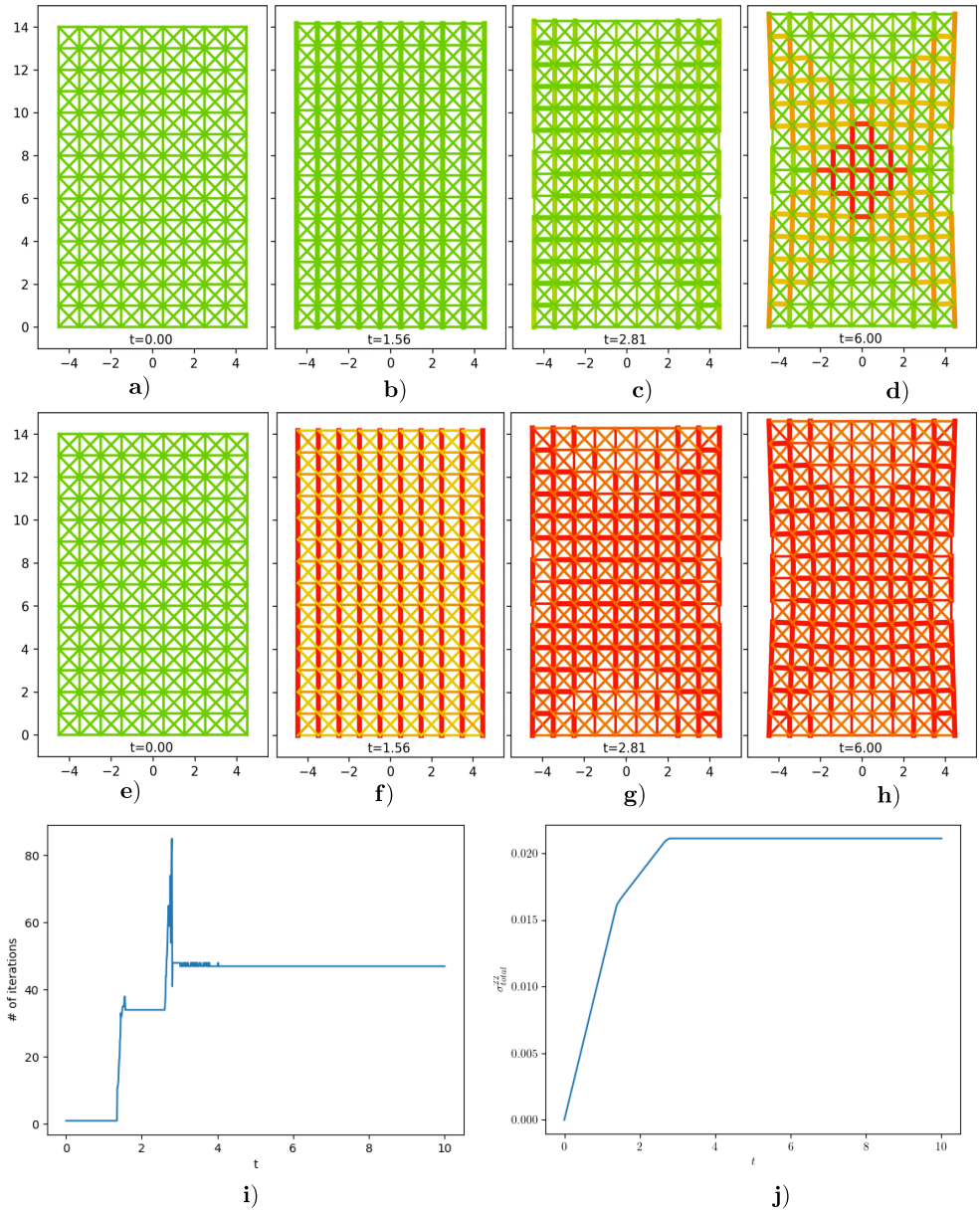

Figure 12. Evolution of a **symmetric** rectangular lattice with **perfect plasticity** under increasing displacement load along the vertical axis (see Section 6.1.3). The presentation is similar to Figure 10.

6.1.4. Lattice with a defect with perfect plasticity

See Figure 13, where all of the springs have the same parameters (6.3), but we introduce a geometric defect into the lattice to destroy its symmetry. Again, the shear band is now formed across the location of the defect (Figure 13d). Unlike the softening case (Figure 10h), there is no unloading at the later stages of the evolution (Figure 13h).

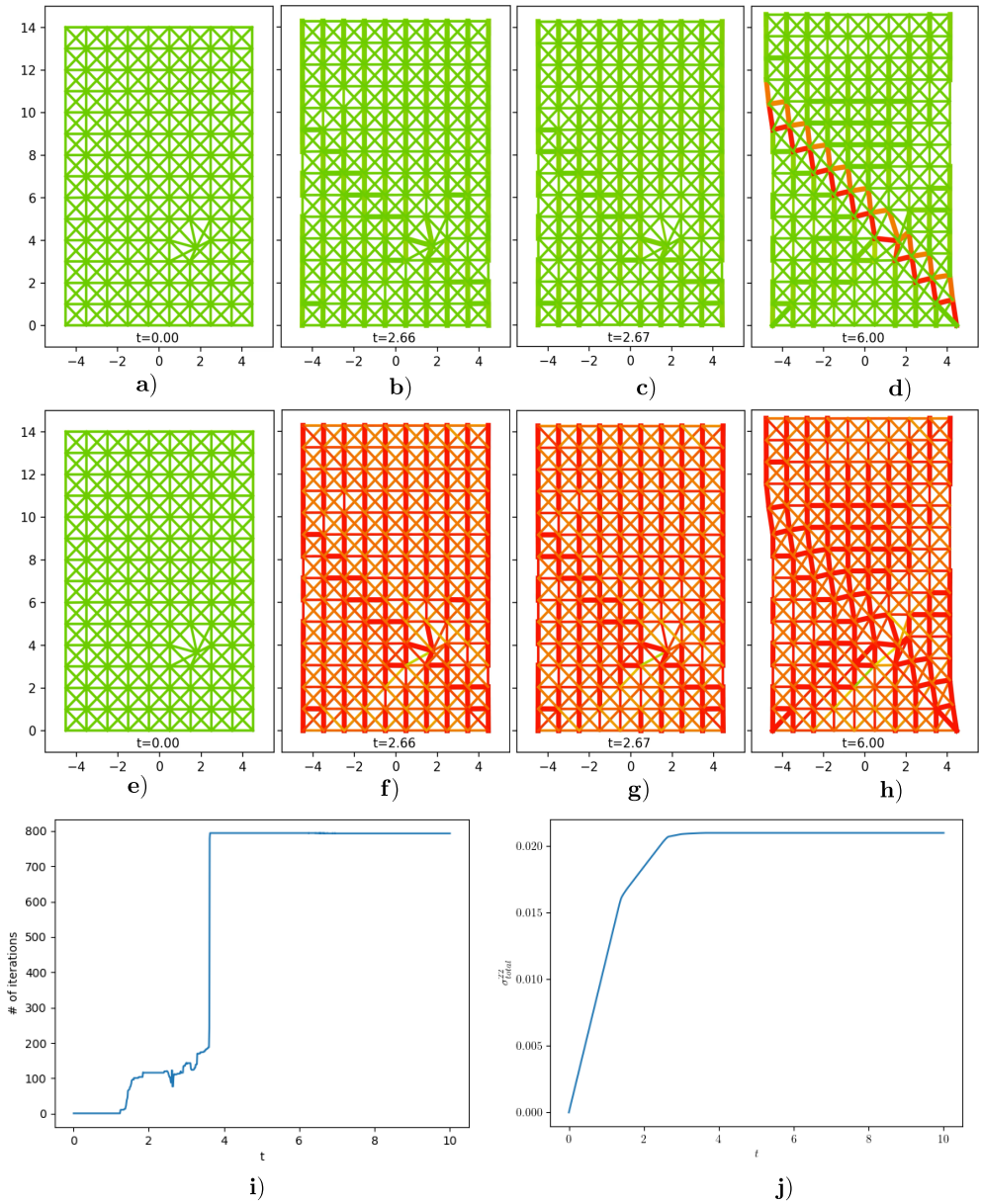

Figure 13. Evolution of a rectangular lattice with a **defect** with **perfect plasticity** under increasing displacement load along the vertical axis (see Section 6.1.4). The presentation is similar to Figure 10.

6.1.5. Symmetric lattice with hardening

See Figure 14, where all of the springs have the following parameters:

$$k_i = 1, \quad h_i = 0.9, \quad s_i = 0.3, \quad c_{0,i} = 0.01, \qquad i \in \overline{1,m}. \tag{6.4}$$

We have obtained a symmetrically distributed solution, similar to the symmetric example with perfect plastcity (Figure 12), but with more plastic deformation. In the case of hardening we know from the theory that the solution is unique for both stresses and displacements.

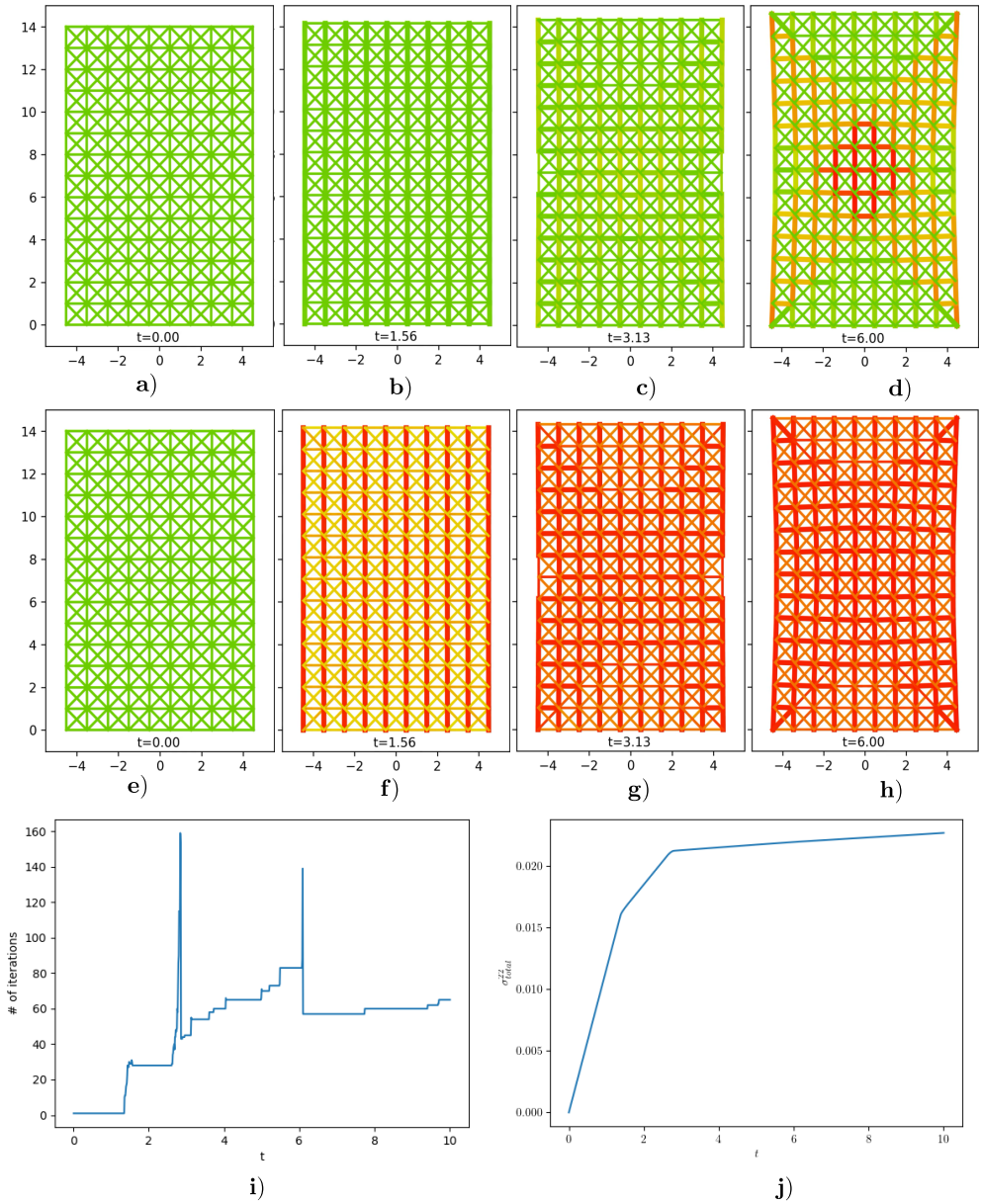

Figure 14. Evolution of a **symmetric** rectangular lattice with **hardening** under increasing displacement load along the vertical axis (see Section 6.1.5). The presentation is similar to Figure 10.

6.1.6. Lattice with a defect with hardening

See Figure 15, where all of the springs have the same parameters (6.4), but we introduce a geometric defect into the lattice to destroy its symmetry.

Notice, that the evolution of the damage has "symmetric" features (Figure 15c,d,f, Figures 12d and 14d, but the localization of damage to the diagonal shear band crossing the defect is still visible (Figure 15c,d).

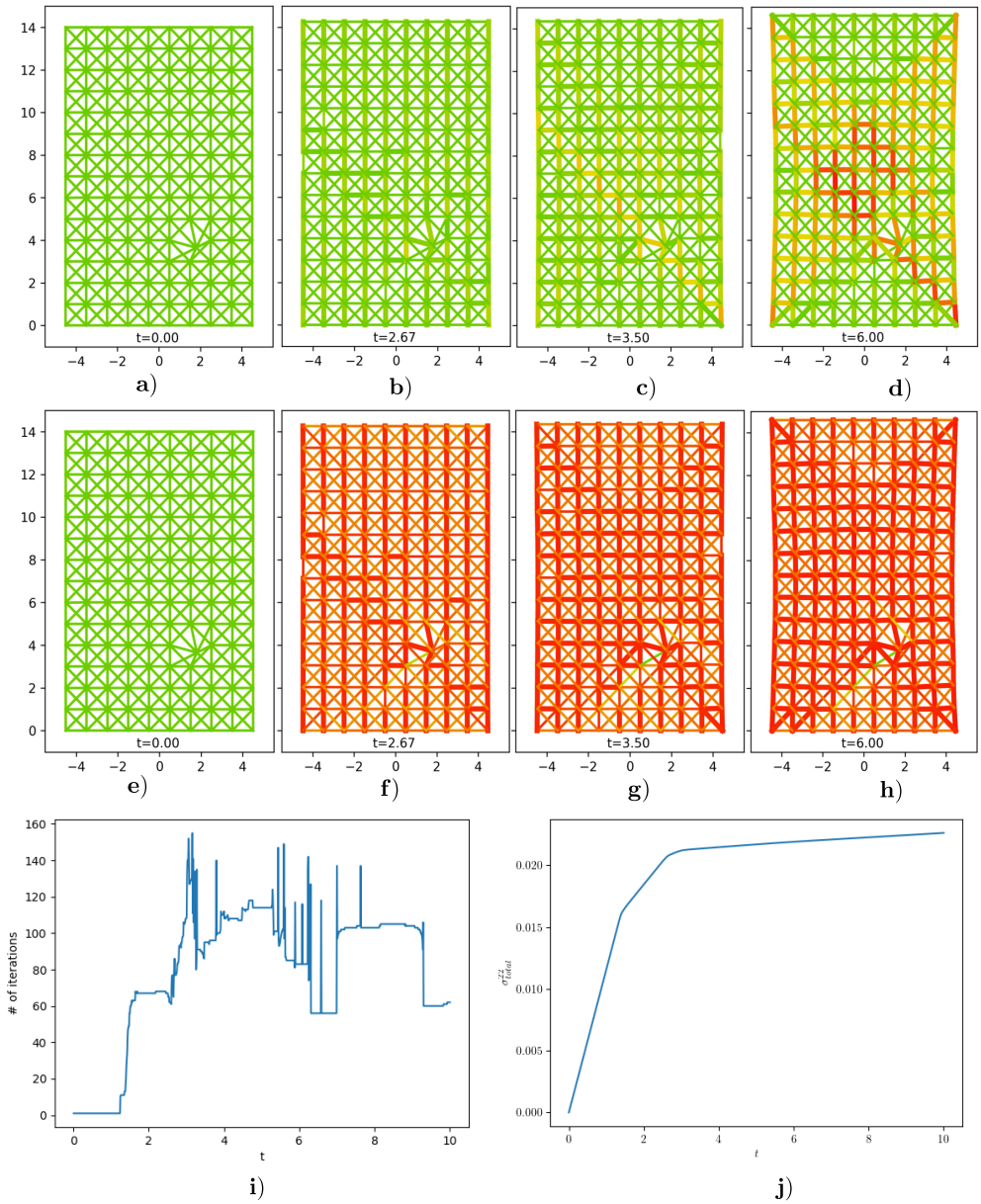

Figure 15. Evolution of a rectangular lattice with a **defect** with **hardening** under increasing displacement load along the vertical axis (see Section 6.1.6). The presentation is similar to Figure 10.

6.2. *Triangular lattice*

Consider now a similar triangular lattice (Figure 16a) under the similar displacement loading along the vertical direction. The following values characterize the lattice:

$$\begin{aligned} \text{number of spatial dimensions:} &\quad d = 2, \\ \text{number of nodes:} &\quad n = 157, \\ \text{number of springs:} &\quad m = 404, \\ \text{number of external displacement constraints:} &\quad q = 21, \\ \text{dimension of the space of self-stresses:} &\quad \dim \mathcal{V} = 111. \end{aligned}$$

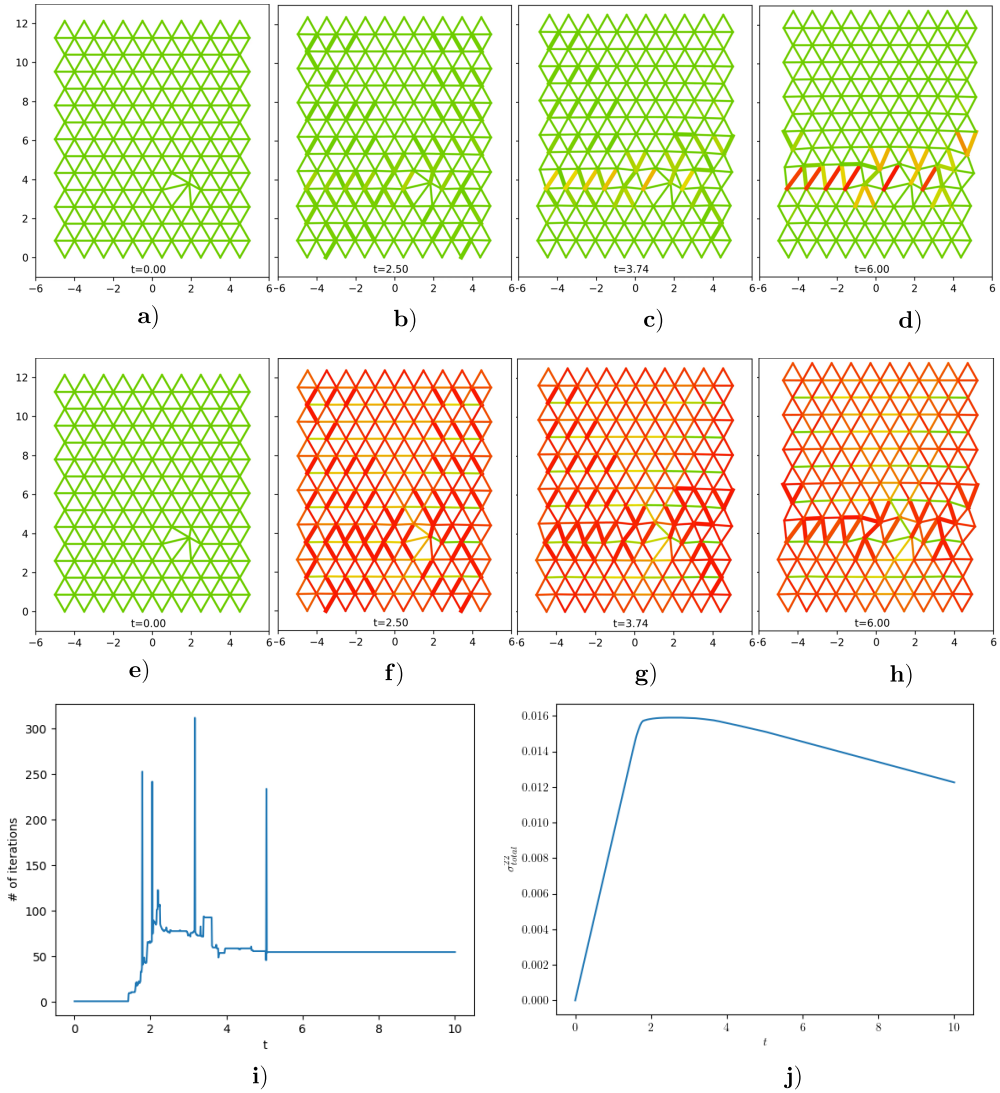

Figure 16. Evolution of a triangular lattice with a defect with softening under increasing displacement load along the vertical axis (see Section 6.2). The presentation is similar to Figure 10.

For the triangular lattice we will only consider the case of defect included and springs with

softening. All of the springs have the following parameters:

$$k_i = 1, \quad h_i = 1.1, \quad s_i = 0.2, \quad c_{0,i} = 0.01, \qquad i \in \overline{1,m}.$$

Similarly to the corresponding example with the rectangular lattice (Figure 11) we observe the localization of damage and displacement into a shear band crossing the defect, and some elastic unloading in the rest of the lattice. However, the shear band is now horizontal, from which we conclude that the model output severely depends on the structure of the lattice.

7. Conclusions and directions for future research

We have proposed a state-dependent sweeping process model of an elastoplastic spring, which may be a hardening, perfectly plastic, or softening spring, depending on the value of the parameter h. Curiously enough, progressive plastic deformation in the model is controlled by two parameters (the coefficient of state-dependent feedback h and the geometric slope s), which naturally arise in the mathematical formulation, while their interplay results in a single observable characteristic, the plasticity modulus E^p of the spring, see (3.17). We will leave it to physicists and engineers to judge if h and s on their own could be interpreted as objective physical properties.

Further, we have explicitly written an analogous state-dependent sweeping process (4.23) for a general Lattice Spring Model, which contains a finite number of such springs. The moving set of such sweeping process is convex, moreover, it is an unbounded *polytpe with fixed directions of the normal vectors to its faces*. The state-dependence of the moving set arises as a trade-off for the non-convexity of the energy function in the variational formulations (see [11, 22, 23, 56]).

We succeeded to numerically solve the state-dependent sweeping process in our examples of LSMs by finding an asymptotically stable fixed point of the map T_j (see (4.56)) for each time-step j of the implicit catch-up algorithm. Such numerical solutions can be computed up to the earliest point of complete failure of the springs.

This is in agreement with the fact that the cornerstone of the theory of state-dependent sweeping process, Theorem 1.2 by Kunze and Monteiro Marques, only covers the case of hardening ($h < 1$), and exactly excludes less trivial cases of perfect plasticity ($h = 1$) and softening ($h > 1$). In the future, we plan to present a local version of the theorem to cover all of the three types and justify the existence of a fixed point for a time-step in the implicit catch-up algorithm, provided that none of the m springs is near the state of complete failure. That would yield a solution to the time-continuous problem by the same argument from the proof of Theorem 1.2.

We have analytically shown the non-uniqueness of solutions in the state-dependent sweeping process of the two-spring model of Figure 1b, and this agrees with the conclusions of [17] on the same model. Moreover, the nonsmooth bifurcation due to softening, which was discussed there and in many other engineering papers, can now be studied within the rigorous mathematical framework of a state-dependent sweeping process.

The importance of our study is backed by the numerical results: as one can see from Figure 8, the simultaneous change of the parameter h across the value 1 for both springs in the toy model dramatically influences the number of fixed points and their stability with respect to the map T_j. In the future, other combinations of the three types of plasticity could be considered to fully understand the stability of the fixed points, as in Figure 8. A complete study of the bifurcation in the two-springs model

may also include the parameters such that $k^{-1}s^2(1-h) < -1$ (see (3.17) and Figure 6) and the reverse direction of loading ($\dot{l} < 0$), which is related to the *snapback* phenomenon [20] and [72, Section 9].

The next open question is to find a method to analytically determine the stability of the fixed points for a general LSM. It is a nontrivial task, as the map T_j is not Fréchet-differentiable (indeed, see (4.56)), and the classical stability analysis via the eigenvalues of the linearization (see, e.g., [78, Section 10.1, pp. 386-387] and [64, Theorem 2.34, p. 239]) is not applicable.

On the other hand, Figure 8 suggests a relation between *numerical stability* of the fixed points (i.e., in terms of the iterated map T_j), and their *mechanical stability*, i.e., their classification as minima, maxima and saddle points of the energy function. It is possible, that the map T_j, which we sourced from the theory behind Theorem 1.2, actually decreases the energy of a state $\begin{pmatrix} y \\ a \end{pmatrix}$ with each iteration, until a local minimum is found. This would mean a deeper connection between variational and sweeping process formulation of the mechanical models. An example with cycling iterations of T_j would, however, disprove this hypothesis.

In our numerical simulations of larger lattices, we have observed emergent formation of shear bands in LSMs with softening, in general agreement with the engineering literature, e.g., [9, 73]. Moreover, in a symmetric lattice with softening the shear band appears as an instantaneous loss of symmetry (Figure 10b,c,f,g), accompanied by a spike in the iterations count of T_j (Figure 10i). We have numerically confirmed non-uniqueness of that solution (cf. Figures 3 and 10d. The orientation of the shear band is sensitive to the defects in the lattice (cf. Figures 10d and 11d and heavily depends on the geometry of the lattice (cf. Figures 11d and 16d. To verify the integral behavior of a lattice as an elasto-plastic body we have computed the evolution of total stress (Figures 10–16j), which reflects the respective type of plasticity.

Naturally, the model we constructed could be adapted to non-isotropic and nonlinear hardening or softening by taking a state-dependent $h(a)$ or more complex (possibly even non-convex) shape of C in (3.4). Instead of the linearization (LSM4) near a fixed reference configuration of the lattice in Section 4.1.2, it is possible to consider evolving geometry of the lattice with "properly rotating" springs, i.e., with the nonlinear state constraint directly defined via the distance function (4.7). Such model would have even more state-dependent terms, in particular, the subspace $\mathcal{V}$ in (4.24). The computational cost in such a model would likely prohibit the implicit catch-up algorithm, at least in its "naive" unoptimized implementation. Other numerical methods for nonsmooth problems [29, 30, 68] may be efficient. However, as we discussed above, stability of the fixed points in the implicit catch-up algorithm reveals the inner properties of the problem itself, thus, the algorithm should not be dismissed even in the presence of faster alternatives.

To mention at last, a similar state-dependent sweeping process formulation of continuous media with softening is conceivable, but it will require measure-valued state variables and appropriately defined governing equations. Such "dual" formulation would be complementary to the existing "primal" variational formulations, as, for example, both formulations together could help with two-sided error estimates, similarly to how it is for linear elliptic problems [51, Theorem 4.4, Figures 4.8 and 4.9, pp. 64–67] and elasticity-perfect plasticity [43]. Moreover, optimal control methods for state-dependent sweeping processes (the current scientific frontier, see, e.g., [3]) may be a way to control the emergence of ductile fractures.

Use of Generative-AI tools declaration

No Generative Artificial Intelligence (Generative-AI) tools were used in the creation of this article.

Acknowledgements

The author thanks Pavel Krejčí from the Institute of Mathematics CAS for helpful scientific discussions.

This research is supported by Czech Science Foundation (GAČR) project GA24-10586S and the Czech Academy of Sciences (RVO: 67985840).

Conflict of interest

The author declares no conflict of interest.

References

1. N. C. Admal, E. B. Tadmor, The non-uniqueness of the atomistic stress tensor and its relationship to the generalized Beltrami representation, *J. Mech. Phys. Solids*, **93** (2016), 72–92. https://doi.org/10.1016/j.jmps.2016.03.016
2. A. Y. Alfakih, *Euclidean distance matrices and their applications in rigidity theory*, Springer, 2018. https://doi.org/10.1007/978-3-319-97846-8
3. H. Antil, R. Arndt, B. S. Mordukhovich, D. Nguyen, C. N. Rautenberg, Optimal control of a quasi-variational sweeping process, *Math. Control Relat. Fields*, **16** (2025), 132–156. https://doi.org/10.3934/mcrf.2025010
4. C. Baiocchi, A. Capelo, *Variational and quasivariational inequalities: applications to free boundary problems*, New York: Wiley, 1984.
5. R. B. Bapat, *Graphs and matrices*, Springer London, 2010. https://doi.org/10.1007/978-1-84882-981-7
6. E. Bauer, V. A. Kovtunenko, P. Krejčí, G. A. Monteiro, L. Paoli, A. Petrov, Non-convex sweeping processes in contact mechanics, *Nonlinear Anal.*, **87** (2026), 104456. https://doi.org/10.1016/j.nonrwa.2025.104456
7. H. H. Bauschke, P. L. Combettes, *Convex analysis and monotone operator theory in Hilbert spaces*, CMS Books in Mathematics, Springer New York, 2011.
8. Z. P. Bazant, Mechanics of distributed cracking, *Appl. Mech. Rev.*, **39** (1986), 675–705. https://doi.org/10.1115/1.3143724
9. R. de Borst, Numerical modelling of bifurcation and localisation in cohesive-frictional materials, *Pure Appl. Geophys.*, **137** (1991), 367–390. https://doi.org/10.1007/BF00879040
10. R. de Borst, L. J. Sluys, H. B. Muhlhaus, J. Pamin, Fundamental issues in finite element analyses of localization of deformation, *Eng. Comput.*, **10** (1993), 99–121. https://doi.org/10.1108/eb023897

11. A. Braides, G. Dal Maso, A. Garroni, Variational formulation of softening phenomena in fracture mechanics: the one-dimensional case, *Arch. Rational Mech. Anal.*, **146** (1999), 23–58. https://doi.org/10.1007/s002050050135

12. H. Brezis, *Functional analysis, Sobolev spaces and partial differential equations*, Springer, 2011. https://doi.org/10.1007/978-0-387-70914-7

13. M. Brokate, P. Krejcí, H. Schnabel, On uniqueness in evolution quasivariational inequalities, *J. Convex. Anal.*, **11** (2004), 111–130.

14. F. C. Campbell, *Elements of metallurgy and engineering alloys*, ASM International, 2008.

15. S. L. Campbell, C. D. Meyer, *Generalized inverses of linear transformations*, Society for Industrial and Applied Mathematics, 2009.

16. C. Castaing, A. G. Ibrahim, M. Yarou, Some contributions to nonconvex sweeping process, *J. Nonlinear Convex Anal.*, **10** (2009), 1–20.

17. G. Chen, G. Baker, Energy profile and bifurcation analysis in softening plasticity, *Adv. Struct. Eng.*, **7** (2004), 515–523. https://doi.org/10.1260/1369433042863224

18. H. Chen, E. Lin, Y. Jiao, Y. Liu, A generalized 2D non-local lattice spring model for fracture simulation, *Comput. Mech.*, **54** (2014), 1541–1558. https://doi.org/10.1007/s00466-014-1075-4

19. J. Clark, D. A. Holton, *A first look at graph theory*, World Scientific, 1991.

20. M. A. Crisfield, Snap-through and snap-back response in concrete structures and the dangers of under-integration, *Int. J. Numer. Methods Eng.*, **22** (1986), 751–767. https://doi.org/10.1002/nme.1620220314

21. G. Dal Maso, A. DeSimone, M. G. Mora, Quasistatic evolution problems for linearly elastic–perfectly plastic materials, *Arch. Rational Mech. Anal.*, **180** (2006), 237–291. https://doi.org/10.1007/s00205-005-0407-0

22. G. Dal Maso, A. DeSimone, M. G. Mora, M. Morini, A vanishing viscosity approach to quasistatic evolution in plasticity with softening, *Arch. Rational Mech. Anal.*, **189** (2008), 469–544. https://doi.org/10.1007/s00205-008-0117-5

23. G. Dal Maso, A. DeSimone, M. G. Mora, M. Morini, Globally stable quasistatic evolution in plasticity with softening, *Netw. Heterog. Media*, **3** (2008), 567–614. https://doi.org/10.3934/nhm.2008.3.567

24. G. Dal Maso, R. Toader, A model for the quasi-static growth of brittle fractures: existence and approximation results, *Arch. Rational Mech. Anal.*, **162** (2002), 101–135. https://doi.org/10.1007/s002050100187

25. A. Demyanov, Regularity of stresses in Prandtl-Reuss perfect plasticity, *Calc. Var.*, **34** (2009), 23–72. https://doi.org/10.1007/s00526-008-0174-5

26. G. Duvant, J. L. Lions, *Inequalities in mechanics and physics*, Grundlehren der mathematischen Wissenschaften, Vol. 219, Springer Berlin, Heidelberg, 1976. https://doi.org/10.1007/978-3-642-66165-5

27. F. Ebobisse, B. D. Reddy, Some mathematical problems in perfect plasticity, *Comput. Methods Appl. Mech. Eng.*, **193** (2004), 5071–5094. https://doi.org/10.1016/j.cma.2004.07.002

28. I. Ekeland, R. Temam, *Convex analysis and variational problems*, Classics in Applied Mathematics, Society for Industrial and Applied Mathematics, 1999. https://doi.org/10.1137/1.9781611971088

29. F. Facchinei, J. S. Pang, *Finite-dimensional variational inequalities and complementarity problems*, Springer Series in Operations Research and Financial Engineering, Springer New York, 2003. https://doi.org/10.1007/b97543

30. P. E. Farrell, M. Croci, T. M. Surowiec, Deflation for semismooth equations, *Optim. Method. Softw.*, **35** (2020), 1248–1271. https://doi.org/10.1080/10556788.2019.1613655

31. G. A. Francfort, A. Giacomini, J. J. Marigo, The elasto-plastic exquisite corpse: a Suquet legacy, *J. Mech. Phys. Solids*, **97** (2016), 125–139. https://doi.org/10.1016/j.jmps.2016.02.002

32. G. A. Francfort, J. J. Marigo, Revisiting brittle fracture as an energy minimization problem, *J. Mech. Phys. Solids*, **46** (1998), 1319–1342. https://doi.org/10.1016/S0022-5096(98)00034-9

33. P. A. Fuhrmann, U. Helmke, *The mathematics of networks of linear systems*, Universitext, Springer Cham, 2015. https://doi.org/10.1007/978-3-319-16646-9

34. G. N. Gatica, *A simple introduction to the mixed finite element method: theory and applications*, SpringerBriefs in Mathematics, Springer Cham, 2014. https://doi.org/10.1007/978-3-319-03695-3

35. H. Goldstein, C. Poole, J. Safko, *Classical mechanics*, 3 Eds., Addison Wesley, 2002.

36. G. Gruben, D. Morin, M. Langseth, O. S. Hopperstad, Strain localization and ductile fracture in advanced high-strength steel sheets, *Eur. J. Mech. - A/Solids*, **61** (2017), 315–329. https://doi.org/10.1016/j.euromechsol.2016.09.014

37. I. Gudoshnikov, Regularity lost: the fundamental limitations and constraint qualifications in the problems of elastoplasticity, *Discrete Cont. Dyn. Syst.*, **51** (2026), 370–438. https://doi.org/10.3934/dcds.2026034

38. I. Gudoshnikov, Y. Jiao, O. Makarenkov, D. Chen, Sweeping process approach to stress analysis in elastoplastic lattice spring models with applications to network materials, *Phys. Rev. E*, **112** (2025), 065501. https://doi.org/10.1103/2jdr-ck1m

39. I. Gudoshnikov, O. Makarenkov, Stabilization of the response of cyclically loaded lattice spring models with plasticity, *ESAIM: Control Optim. Calc. Var.*, **27** (2021), S8. https://doi.org/10.1051/cocv/2020043

40. A. L. Gurson, Continuum theory of ductile rupture by void nucleation and growth: Part I—Yield criteria and flow rules for porous ductile media, *J. Eng. Mater. Technol.*, **99** (1977), 2–15. https://doi.org/10.1115/1.3443401

41. T. Haddad, Differential inclusion governed by a state dependent sweeping process, *Int. J. Difference Equ.*, **8** (2013), 63–70.

42. W. Han, B. D. Reddy, *Plasticity: mathematical theory and numerical analysis*, 2 Eds., Vol. 9, Interdisciplinary Applied Mathematics, Springer New York, 2013. https://doi.org/10.1007/978-1-4614-5940-8

43. J. Haslinger, S. Sysala, S. Repin, Inf–sup conditions on convex cones and applications to limit load analysis, *Math. Mech. Solids*, **24** (2019), 3331–3353. https://doi.org/10.1177/1081286519843969

44. M. Jirásek, Mathematical analysis of strain localization, *Rev. Eur. Génie Civ.*, **11** (2007), 977–991. https://doi.org/10.1080/17747120.2007.9692973

45. M. Jirasek, S. Rolshoven, Regularized formulations of strain-softening plasticity, In: D. Kolymbas, *Advanced mathematical and computational geomechanics*, Lecture Notes in Applied and Computational Mechanics, Springer, Berlin, Heidelberg, **13** (2003), 269–299. https://doi.org/10.1007/978-3-540-45079-5_11

46. M. Kamenskii, O. Makarenkov, L. N. Wadippuli, A continuation principle for periodic BV-continuous state-dependent sweeping processes, *SIAM J. Math. Anal.*, **52** (2020), 5598–5626. https://doi.org/10.1137/19M1248613

47. A. M. Khludnev, V. A. Kovtunenko, *Analysis of cracks in solids*, Advances in Fracture Mechanics Series, WIT Press, 2000.

48. P. Krejčí, G. A. Monteiro, V. Recupero, Explicit and implicit non-convex sweeping processes in the space of absolutely continuous functions, *Appl. Math. Optim.*, **84** (2021), 1477–1504. https://doi.org/10.1007/s00245-021-09801-8

49. P. Krejčí, G. A. Monteiro, V. Recupero, Viscous approximations of non-convex sweeping processes in the space of regulated functions, *Set-Valued Var. Anal.*, **31** (2023), 34. https://doi.org/10.1007/s11228-023-00695-y

50. P. Krejčí, J. Sprekels, Elastic–ideally plastic beams and Prandtl–Ishlinskii hysteresis operators, *Math. Methods Appl. Sci.*, **30** (2007), 2371–2393. https://doi.org/10.1002/mma.892

51. M. Křížek, P. Neittaanmäki, *Mathematical and numerical modelling in electrical engineering theory and applications*, Mathematical Modelling: Theory and Applications, Vol. 1, Springer Dordrecht, 1996. https://doi.org/10.1007/978-94-015-8672-6

52. M. Kunze, M. D. P. Monteiro Marques, An Introduction to Moreau's sweeping process, In: B. Brogliato, *Impacts in mechanical systems*, Lecture Notes in Physics, Springer, Berlin, Heidelberg, **551** (2000), 1–60. https://doi.org/10.1007/3-540-45501-9_1

53. M. Kunze, M. D. P. Monteiro Marques, On parabolic quasi-variational inequalities and statedependent sweeping processes, *Topol. Methods Nonlinear Anal.*, **12** (1998), 179–191.

54. A. Lemaître, Inherent stress correlations in a quiescent two-dimensional liquid: static analysis including finite-size effects, *Phys. Rev. E*, **96** (2017), 052101. https://doi.org/10.1103/PhysRevE.96.052101

55. T. C. Lubensky, C. L. Kane, X. Mao, A. Souslov, K. Sun, Phonons and elasticity in critically coordinated lattices, *Rep. Prog. Phys.*, **78** (2015), 073901. https://doi.org/10.1088/0034-4885/78/7/073901

56. M. Lambrecht, C. Miehe, J. Dettmar, Energy relaxation of non-convex incremental stress potentials in a strain-softening elastic–plastic bar, *Int. J. Solids Struct.*, **40** (2003), 1369–1391. https://doi.org/10.1016/S0020-7683(02)00658-3

57. J. A. C. Martins, M. D. P. Monteiro Marques, A. Petrov, On the stability of quasi-static paths for finite dimensional elastic-plastic systems with hardening, *Z. Angew. Math. Mech.*, **87** (2007), 303–313. https://doi.org/10.1002/zamm.200510315

58. C. Meng, Y. Liu, Damage-augmented nonlocal lattice particle method for fracture simulation of solids, *Int. J. Solids Struct.*, **243** (2022), 111561. https://doi.org/10.1016/j.ijsolstr.2022.111561

59. A. Mielke, T. Roubíček, *Rate-independent systems: theory and application*, Applied Mathematical Sciences, Springer New York, 2015. https://doi.org/10.1007/978-1-4939-2706-7

60. M. G. Mora, Relaxation of the Hencky model in perfect plasticity, *J. Math. Pures Appl.*, **106** (2016), 725–743. https://doi.org/10.1016/j.matpur.2016.03.009

61. J. J. Moreau, Application of convex analysis to the treatment of elastoplastic systems, In: P. Germain, B. Nayroles, *Applications of methods of functional analysis to problems in mechanics*, Lecture Notes in Mathematics, Springer, Berlin, Heidelberg **503** (1976), 56–89. https://doi.org/10.1007/BFb0088746

62. J. J. Moreau, Evolution problem associated with a moving convex set in a Hilbert space, *J. Differ. Equations*, **26** (1977), 347–374. https://doi.org/10.1016/0022-0396(77)90085-7

63. J. J. Moreau, On unilateral constraints, friction and plasticity, In: G. Capriz, G. Stampacchia, *New variational techniques in mathematical physics*, C.I.M.E. Summer Schools, Springer, Berlin, Heidelberg, **63** (1974), 171–322. https://doi.org/10.1007/978-3-642-10960-7_7

64. J. Müller, C. Kuttler, *Methods and models in mathematical biology: deterministic and stochastic approaches*, Lecture Notes on Mathematical Modelling in the Life Sciences, Springer Berlin, Heidelberg, 2015. https://doi.org/10.1007/978-3-642-27251-6

65. J. Nečas, I. Hlaváček, *Mathematical theory of elastic and elasto-plastic bodies: an introduction*, Studies in Applied Mechanics, Elsevier, 1981.

66. A. Needleman, V. Tvergaard, An analysis of ductile rupture in notched bars, *J. Mech. Phys. Solids*, **32** (1984), 461–490. https://doi.org/10.1016/0022-5096(84)90031-0

67. P. J. Olver, C. Shakiban, *Applied linear algebra*, 2 Eds., Undergraduate Texts in Mathematics, Springer Cham, 2018. https://doi.org/10.1007/978-3-319-91041-3

68. J. Outrata, M. Kocvara, J. Zowe, *Nonsmooth approach to optimization problems with equilibrium constraints: theory, applications and numerical results*, Nonconvex Optimization and Its Applications, Vol. 28, Springer, 2013.

69. G. Pijaudier-Cabot, Z. P. Bažant, M. Tabbara, Comparison of various models for strainsoftening, *Eng. Comput.*, **5** (1988), 141–150. https://doi.org/10.1108/eb023732

70. J. Rigelesaiyin, A. Diaz, W. Li, L. Xiong, Y. Chen, Asymmetry of the atomic-level stress tensor in homogeneous and inhomogeneous materials, *Proc. A*, **474** (2018), 20180155. https://doi.org/10.1098/rspa.2018.0155

71. R. T. Rockafellar, *Convex Analysis*, Princeton: Princeton University Press, 1970. https://doi.org/10.1515/9781400873173

72. J. G. Rots, R. de Borst, Analysis of concrete fracture in "direct" tension, *Int. J. Solids Struct.*, **25** (1989), 1381–1394. https://doi.org/10.1016/0020-7683(89)90107-8

73. S. A. Sabet, R. de Borst, Structural softening, mesh dependence, and regularisation in non-associated plastic flow, *Int. J. Numer. Anal. Methods Geomech.*, **43** (2019), 2170–2183. https://doi.org/10.1002/nag.2973

74. B. Satco, G. Smyrlis, State-dependent sweeping processes with Stieltjes derivative, *Appl. Math. Optim.*, **90** (2024), 24. https://doi.org/10.1007/s00245-024-10169-8

75. H. C. Schnabel, *Zur Wohlgestelltheit des Gurson-Modells*, Ph.D. Thesis, Technische Universitat Munchen, 2006.

76. J. C. Simo, T. J. R. Hughes, *Computational inelasticity*, Interdisciplinary Applied Mathematics, Vol. 7, Springer New York, 1998. https://doi.org/10.1007/b98904

77. G. Strang, H. Matthies, R. Temam, Mathematical and computational methods in plasticity, In: S. Nemat-Nasser, *Variational methods in the mechanics of solids*, Proceedings of the IUTAM Symposium on Variational Methods in the Mechanics of Solids Held at Northwestern University, Evanston, Illinois, 1980, 20–28. https://doi.org/10.1016/B978-0-08-024728-1.50008-2

78. S. H. Strogatz, *Nonlinear dynamics and chaos: with applications to physics, biology, chemistry, and engineering*, 3 Eds., CRC Press, 2024.

79. Supplemental material: videos and computer programs of simulations can be found at `https://github.com/Ivan-Gudoshnikov/Elastoplasticity-softening-public`.

80. P. M. Suquet, Discontinuities and plasticity, In: J. J. Moreau, P. D. Panagiotopoulos, *Nonsmooth mechanics and applications*, International Centre for Mechanical Sciences, **302** (1988), 279–340. https://doi.org/10.1007/978-3-7091-2624-0_5

81. P. M. Suquet, Existence and regularity of solutions for plasticity problems, In: S. Nemat-Nasser, *Variational methods in the mechanics of solids*, Proceedings of the IUTAM Symposium on Variational Methods in the Mechanics of Solids Held at Northwestern University, Evanston, Illinois, 1980, 304–309. https://doi.org/10.1016/B978-0-08-024728-1.50053-7

82. P. M. Suquet, Sur les équations de la plasticité: existence et régularité des solutions, *J. Mécanique*, **20** (1981), 3–39.

83. P. M. Suquet, Sur un nouveau cadre fonctionnel pour les équations de la plasticité, *C. R. Acad. Sci. Paris Ser.*, **286** (1978), 1129–1132.

84. R. Temam, *Mathematical problems in plasticity*, Modern Applied Mathematics Series, Trans-Inter-Scientia, 1985.

85. R. Temam, G. Strang, Functions of bounded deformation, *Arch. Rational Mech. Anal.*, **75** (1980/81), 7–21. https://doi.org/10.1007/BF00284617

86. V. Tvergaard, Material failure by void growth to coalescence, *Adv. Appl. Mech.*, **27** (1989), 83–151. https://doi.org/10.1016/S0065-2156(08)70195-9

87. H. Van Swygenhoven, P. M. Derlet, Chapter 81–Atomistic simulations of dislocations in FCC metallic nanocrystalline materials, *Dislocat. Solids*, **14** (2008), 1–42. https://doi.org/10.1016/S1572-4859(07)00001-0

AIMS Press